North Carolina Agricultural and Technical State University

Aggie Digital Collections and Scholarship

Theses   Electronic Theses and Dissertations

2013

Biocompatibility Of Magnesium-Based Biomaterials For Airway Stent Applications

Sara Dolly Tatum
North Carolina Agricultural and Technical State University

Follow this and additional works at: https://digital.library.ncat.edu/theses

Biocompatibility of Magnesium-Based Biomaterials for Airway Stent Applications

Sara Dolly Tatum

North Carolina A&T State University

A thesis submitted to the graduate faculty

in partial fulfillment of the requirements for the degree of

MASTER OF SCIENCE

Department: Biology

Major: Biology

Co-Advisors: Dr. Jenora Waterman and Dr. Patrick Martin

Greensboro, North Carolina

2013

School of Graduate Studies
North Carolina Agricultural and Technical State University
This is to certify that the Master's Thesis of

Sara Dolly Tatum

has met the thesis requirements of
North Carolina Agricultural and Technical State University

Greensboro, North Carolina
2013

Approved by:

_____   _____
Dr. Jenora T. Waterman   Dr. Patrick Martin
Co-Advisor   Co-Advisor

_____   _____
Dr. Gregory Goins   Dr. Mary Smith
Committee Member   Department Chair

_____
Dr. Sanjiv Sarin
Dean, The Graduate School

Biographical Sketch

Sara Dolly Tatum was born January 11, 1989 in Denver, Colorado. She received a Bachelor of Science in Biology from Bennett College located in Greensboro, North Carolina in 2011. She is a candidate for a Master's of Science in Biology.

Dedication

I would like to first thank God for with him I am able to conquer all. I dedicate this thesis to my loving parents Kevin and Robin Harmon-Tatum, my brother Kelly Tatum, his lovely wife Nicky and my beautiful nieces Zoey and Jordyn, my grandparents Sara "Nene" Harmon, Ezekiel Harmon, James Donald Tatum and Claudine Owens. In addition I would like to thank my all of my family and friends that have continued to support me throughout my educational process.

Acknowledgements

Foremost, I would like to acknowledge my lord and savior Jesus Christ whom without I would not be able to embark on the journey to completing a Master's of Science degree. Secondly, I would like to thank my very loving family and friends who have encouraged me to excel throughout this process. I am thankful for Dr. Jenora Waterman for her dedication and commitment to my educational endeavors. I want to acknowledge my committee members Dr. Goins and Dr. Martin for leading me to success. Also, I would like to thank Drs. Xu and Gilbert for their kind gifts. I am also thankful for the National Science Foundation, the Engineering Research Center and Dr. Sankar for funding my research. Finally, I would like to thank my wonderful lab mates and fellow graduate colleagues. We are an amazing team, wonderful friends and I am truly honored to have shared this time with each of you.

Table of Contents

List of Figures

List of Tables

Key to Symbols and Abbreviations

NF- κB   Nuclear Factor kappa B

iNOS   inducible Nitric Oxide Synthase

SOD   Superoxide Dismutase

GST   Glutathione S Transferase

PI- κB   Phosphorylated Inhibitor of κB

RT-PCR   Reverse Transcriptase- Polymerase Chain Reaction

RPM   Revolutions Per Minute

TBS-T   Tris Buffered Saline-Tween

Kb   kilobases

dNTP   deoxynucleotide triphosphate

kDa   kilodaltons

ECL   Enhanced Chemiluminescence

TAQ   *Thermophilus aquaticus*

SDS-PAGE   Sodium Dodecyl Sulfate Polyacrylamide Gel Electrophoresis

κ   kappa

NHBE   Normal Human Bronchial Epithelial

Pen-Strep   Penicillin-Streptomycin

AmphoB   Amphotericin B

ml   milliliter

μl   microliter

PBS   Phosphate Buffered Saline

EGF   Epidermal Growth Factor

Abstract

Tracheomalacia, stenosis and other traumatic airway injuries (e.g., obstructive tracheobronchial tumors) often require airway stenting. Traditional polymeric stents are prone to cause infection, do not 'grow' with a child and often require surgical removal. Therefore, resorbable biometallics are ideal materials for tracheal stent devices. Magnesium (Mg) is an attractive material because of its biocompatibility, abundance within the human body, and intrinsic corrosive nature can be overcome via alloying elements. We hypothesize that resorbable magnesium-based materials can be utilized for the development of tracheal stents. The objective of the present study was to determine cytocompatibility of Mg alloys with fully differentiated cultures of normal human bronchial epithelial (NHBE) cells to simulate an *in vivo* response. Confluent cultures of differentiated NHBE cells were exposed to wires of high purity Mg or novel MgZnCa alloy for 0,4,18, 24, and 48 hours. Endpoint assays included reverse transcriptase PCR, western blot analysis, and ELISA to assess modulation of cellular responses such as regulation of inflammatory mediators and mucus secretion; wire corrosion was evaluated via scanning electron microscopy. A wound repair assay was performed to evaluate the effect of wires on cell proliferation. One-way analysis of variance (ANOVA) and Bonferroni post-test corrections (p-value<0.05) were performed to detect differences among means. Wires of MgZnCa did not elicit inflammation, inhibit cell proliferation or migration; and degraded less than Mg wires. These findings suggest MgZnCa alloy may be an acceptable biomaterial to use in the application of tracheal stents; however, further analysis is required to determine long-term stent-airway dynamics

CHAPTER 1

Introduction

Airway obstruction, caused by tracheal stenosis or tracheomalacia (especially in children and infants), is a pressing problem that requires an involved solution. For these ailments, common treatments range from balloon dilations to traditional surgical treatments (including the stabilization of airway lumen through implanting a metallic or silicone stents) to invasive surgical procedures (slide tracheoplasty in children or surgical resection of the trachea with primary reconstruction).   The use of metal stent implants has been met with controversy due to the physiological and technical difficulties associated with toxicity and inflammation; however, some benefits have been attained (Michel, 2000). Development of obstructive granulation tissue (Pahl, 1999), possible toxicity due to corrosion or leaching (Poynter, 2003), recovery difficulties (Patel, 2006) and lack of biocompatibility (Yuen, 2010) have been reported as the major issues encountered with the use of metallic stents. Even though the challenges of metallic stent use seem insurmountable, their benefits outweigh their inadequacies. Metallic stents have been found to provide smaller migration rates, add conformity to abnormal airways, increase cross-sectional airway diameters, and add inner stent epithelialization enabling mucociliary clearance (Patel, 2006). The research in this project is therefore important as it is evident that metallic stents are valuable tools in the treatment of airway strictures, but so far, the ideal stent has yet to be designed.

1.1 Magnesium's functions and biocompatibility in the human airway.

The long-term goal is to utilize magnesium (Mg) alloys for resorbable tracheal stent devices. Magnesium is an attractive material because of its biodegradability and biocompatibility. Magnesium is an essential divalent intracellular cation that plays a pivotal role

in daily physiological functions within the body. In fact, magnesium is necessary for the synthesis of nucleic acids and proteins, and is critical in the production and function of various enzymes and transporters (Poynter, 2003). There are approximately 22-26 grams (1 mole) of magnesium within the adult human body and it is the fourth most abundant cation (Adcock, 2006). Mg also has important effects on the body's cardiovascular system (Adcock, 2006), as well as modulation of neuromuscular transmissions (Jones, 2004). Additionally, Mg does not inhibit cell growth and enhances bone cell adhesion (Yuen, 2010). Magnesium, along with calcium, act in concert within the human airway to control smooth airway muscle (Gourgoulianis, 2001). The electroneutral calcium efflux pump found in the plasma membrane of most cells including airway smooth muscle, is a magnesium and ATP dependent enzyme, which extrudes one calcium ion for two hydrogen ions (Knox, 1995). It is stimulated by calcium-calmodulin complex that may act as a feedback mechanism to limit the rise in intracellular calcium following stimulation (Knox, 1995). Although magnesium is subject to corrosion, its corrosion resistance can be improved by alloying it with other less corrosive metals such as titanium or zinc.

1.2 Innovation.

The goal of this study is to evaluate cell physiology and cytotoxic potential of NHBE cells following exposure to magnesium alloy wires. An air-liquid interface (ALI) cell culturing system is used as a model because NHBE cells maintained in this manner are essentially identical to tracheal epithelial cells *in vivo* with respect to structure and function. In addition, this model reduces the occurrence of magnesium corrosion due to the lack of wire submersion in the cell culture medium.

1.3 Applications of Biomaterials.

The field of tissue engineering and regenerative medicine has increased greatly due to the development and incorporation of biocompatible and bioactive materials. More specifically, biomaterials have contributed to this growth due to their dynamic properties useful in various applications such as wound healing, drug delivery (Zhang, 2010) and tissue scaffolds (Kumar, 2009). However, in order for this revolution to continue, the safety and toxicity of these novel materials must be properly investigated. This study will evaluate the efficacy of magnesium alloy wires as a material for scaffolding in the development of biodegradable tracheal stents.

CHAPTER 2

Literature Review

Diseases that affect the trachea such as congenital tracheomalacia (in infants), tracheal stenosis and other obstructive airway disorders caused by injury, all require a complex solution. Currently there are permanent stents that often require surgical insertion and removal (Purnama, 2010). A novel alternative to these permanent stents are biodegradable, biocompatible, biometal stents. Precise knowledge about tissue-implant interactions, tissue engineering, regenerative medicine as well as recent advances in cell and molecular biology have given rise to the new concept of bioactive materials. Unlike conventional inert biometals, bioactive materials are supposed to promote positive interactions with physiological implantation sites (Purnama, 2010).

Degradable biomaterials constitute a novel class of highly bioactive biomaterials that are expected to support the healing process of a diseased tissue or organ and subsequently degrade at a rate proportional to regeneration. Studying novel degradable biomaterials is currently one of the most interesting research topics in biomaterials. Advances in materials science and engineering, in particular concerning processing and thermomechanical treatment, allow the properties of these structural materials to be tailored for specific applications (Purnama, 2010). The demand for biomaterialists to develop new technologies and provide better implants with higher clinical performance has been substantially increased by the ever-aging society and a push for a better quality of life. The old paradigm that states implants must be inert and corrosion resistant has been shifted via the introduction of this new class of biomaterials. This set includes two classes of materials identified by the term "permanent" and "degradable" in reference to corrosion resistant biomaterials.

Biodegradable biomaterials have been proposed since 1988 including polymers such as poly-$_L$-lactic-acid (PLLA), polyglycolic acid/polylactic acid and polycaprolactone. The research for degradable magnesium alloys and related materials started in the 1900's and 1920's (Yuen, 2010). In 1938 magnesium was used in a degradable metallic material (DMM) to fix bone fractures (Purnama, 2010); however, the main issue with DMM's is that they induce local or systemic toxicity (Purnama, 2010). In spite of the vast potential of magnesium biometals, rapid degradation rates may impose severe limitations in clinical applications thus necessitating incorporation of biocompatible alloying elements (Xin, 2011). A brief summary of current literature related to respiratory pathology, magnesium biocompatibility and airway stenting is presented here.

2.1 The Respiratory System and Tracheal Pathophysiology

The process of metabolism in the human body consumes oxygen and produces the waste product carbon dioxide. The cardinal function of the respiratory system is to exchange the carbon dioxide accumulated in the blood for oxygen in the airways via the nose, pharynx, larynx, trachea and bronchi.

There are two functional components of the respiratory system: the conducting zone and the respiratory zone. The conducting zone works to bring air into the lungs and exists both outside and inside the lungs. Components of the conducting zone are the nose, pharynx, larynx, trachea, bronchi and the bronchioles. The respiratory zone is the site of gas exchange and consists of the respiratory bronchioles, alveolar ducts, alveolar saccules and alveoli (Gray, 1918). The ribcage is an airtight cylinder with the diaphragm as the base and the root of the neck as the top lid. Inspiration (inhalation) is always an active process mainly involving muscular contraction of the diaphragm and intercostals muscles (Marieb, 2010). Expiration is typically a

passive process caused primarily by elastic recoil of the diaphragm and relaxation of the intercostals muscles.

The trachea descends from the larynx through the neck and into the mediastinum and ends by dividing into the two main bronchi at mid thorax and enters the lungs. The trachea is chiefly a stack of horseshoe (or "C") shaped cartilaginous rings that are connected to each other by fibrous tissue, forming a "gutter" opening at the backside that is closed by the trachealis muscle that connects to the ends of the "C" shaped rings. The number of cartilage rings in the trachea can vary from sixteen to twenty in number. Each ring forms an imperfect circle and measures about 4mm in depth and 1mm in thickness. These cartilages are stacked on top of each other horizontally and separated by narrow intervals. Their outer surfaces are flattened in a vertical direction; however, being thicker in the middle than at the margins, they are internally convex. The cartilages remain highly elastic in early and mid-life but, may become calcified in advanced life (Gray, 1918).

The trachea is about 10-12cm long, approximately 2cm in diameter, very flexible and mobile. The walls consist of the mucosa, submucosa, adventitia and a layer of hyaline cartilage. The mucosa is lined with goblet cell containing pseudostratified epithelium that is prevalent in most of the respiratory tract. The cilia are essential as it persistently sweeps debris-laden mucus toward the pharynx. The submucosa is composed of a network of loose connective tissue that contains large blood vessels, nerves and mucous glands; the ducts of the aforementioned overlay layers and open on the surface and help produce mucus "sheets" in the trachea. The submucosa is located deep to the mucosa. The submucosa is supported by sixteen to twenty "C" shaped rings of hyaline cartilage encased by the adventitia that is the outermost layer of connective tissue.

The elasticity of the trachea makes it flexible enough to stretch during inspiration and recoil during expiration. Tracheal rings prevent the trachea from collapsing and keep the airway patent despite pressure changes that occur during breathing. The trachealis muscle connects the open posterior parts of the cartilage rings that lie alongside the esophagus. Since this portion of the trachea is not rigid the esophagus can expand anteriorly so that swallowed food can move through. When the trachealis muscle contracts it decreases the diameter of the trachea and forces expired air to rush upward from the lungs with greater force (cough). The final tracheal cartilage is called the carina. The carina is thick and broad in the middle and projects posteriorly from its inner face, marking the point where the trachea branches into the two main bronchi. The mucosa of the carina is very sensitive and in the presence of foreign objects causes violent coughing. When inhaled air reaches the end of the trachea it is clean, warm and saturated with water vapor.

2.1.1 Tracheal Obstruction

Since the trachea is the normal route for air entry into the lungs, tracheal obstruction is life threatening. Pulmonary irritant reflexes respond to inhaled irritants in the nasal passages or trachea by causing reflexive bronchoconstriction in the respiratory airways (Marieb, 2010). Tracheal obstruction can be caused by a myriad of threats. Infants up to 2-3 months of age are obligatory nose breathers and are unable to breathe in through their mouth; therefore, nasal congestion in infants is severe. Tracheobronchial cartilaginous rings of the young child can collapse easily, such that external compression or a slight increase in negative force will cause tracheal collapse (Hoffer, 1994).

Tracheomalacia, on the other hand, is described as weakness of the cartilaginous rings of the trachea. Tracheomalacia is encountered in both pediatric and adult medicine. Malacia, in medical terminology, is described as "a morbid softening or softness of a tissue or part"

(Leonard, 1997). The softness generally refers to bone or in this case the cartilage of the trachea. Tracheomalacia is typically due to a reduction and/or atrophy of the longitudinal elastic fibers of the pars membranacea or impaired cartilage integrity such that the airway is softer and more susceptible to collapse.

Tracheal stenosis is characterized by structural tracheal constriction. It presents in long or short segments and is associated with pulmonary, cardiovascular and gastrointestinal malformations (Ho, 2008). In infants tracheal stenosis is typically congenital; in adults however; stenosis can be caused by trauma, a chronic inflammatory disease, a benign or malignant neoplasia or a collagen vascular disease (Carden, 2005). Events leading to stenosis in adults include; ulceration of the mucosa and cartilage, inflammatory reactions with associated granulation tissue, fibrous tissue formation and contraction of fibrous scar tissue (Carden, 2005). Healing of ulceration (the earliest of laryngotracheal injury that is produced by an enodotracheal tube) involves regeneration of the epithelium (primary healing) or repair (secondary healing). If the granulation tissue is not covered by regenerated epithelium, then the granulation tissue will become exaggerated (Carden, 2005). Granulation tissue which is, new connective tissue and tiny blood vessels that form on the surfaces of a wound during the healing process, may be the most common problem and risks obstructing already unstable, narrowed lumen (Ho, 2008).

2.2 Current Airway Stents

Current trends in airway repair include a large facet of repair techniques. Tracheobronchial prostheses or airway stents are used to palliate the effects of large airway obstruction (Saito, 2005). Airway stenting can be complementary to open surgical treatment in some settings and may replace the need for surgery completely. In patients with airway obstruction caused by advanced malignant disease, airway stenting can produce a gratifying

improvement in quality of life and prevent death from an obstructed airway (Saito, 2005). A variety of stents have been studied experimentally and/or used clinically to aid in the management of complex tracheal, cranial and bronchial stenoses (Jacobs, 2000). Airway stents resemble finger cuffs initially; they are small, intricate devices that are pleasing to the eye but have potential for unforeseen complications. These stents have gained increasing popularity in the management of difficult airway obstructions based on the simplicity of their placement and the lack of good alternative approaches. Also, careful and judicious stent placement has provided significant and life-saving airway improvement in many patients (Zakaluzny, 2003).

In general, airway stents can be classified into one of four categories; silicone, balloon dilated metal stent, self-expanding metal stent and covered self-expanding metal stent (Chin, 2008). Silicone stents are derived from the Montgomery T-tube originally described in the 1960's (Chin, 2008). The T-tube design has been modified by several pulmonologists and surgeons creating the Dumon, Hood, Reynders, Dynamic and Polyflex subtypes (Figure 1). In contrast to the silicone stents, early metal airway stents were developed from endovascular stent technology (Figure 2). The metal is usually stainless steel, cobalt- alloys, titanium-alloys and/or nitinol (Xin, 2008). The most common complications associated with airway stents are migration of the stent, granulation tissue formation around the stent and diminished mucociliary clearance, poor patient tolerance, problems with placement and removal. Therefore, the biodegradable stent proposed in this research study is a necessary first step toward addressing these complications.

Migration is one of the most frequent complications associated with the use of stents, it is essentially vital that the stent remains stationary after being placed. Silicone stents are more prone to migration and may even be expelled. Migration is less common in metallic stents because of the method of deployment used and the inherent properties of the stent.
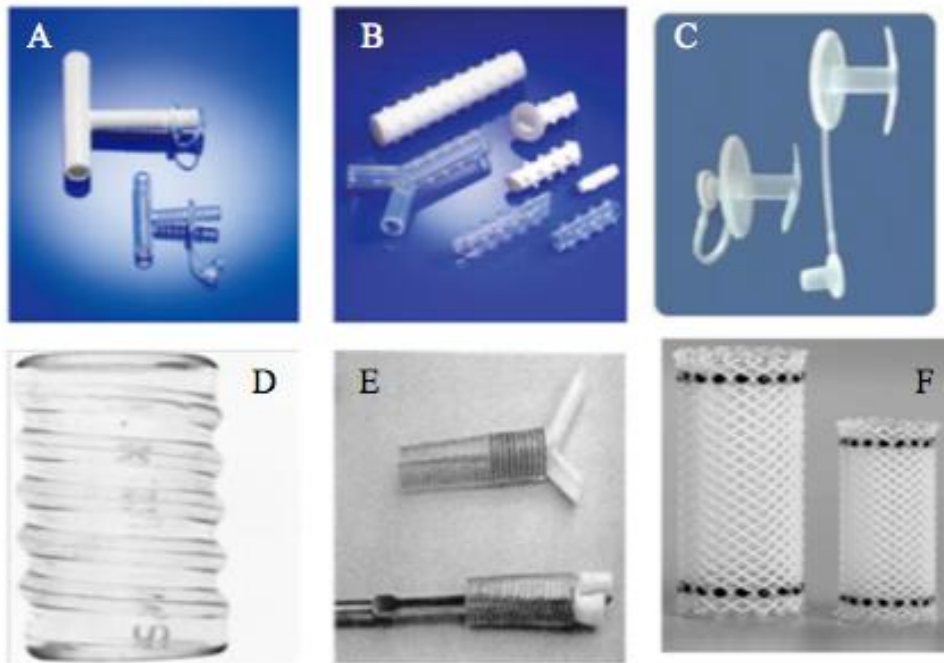
Figure 1 Current silicone airway stents. (A) Montgomery T-tube (Healthcare, 2013), (B) Dumon Silicone tubes (Novatech, 2013), (C) Hood silicone stent (Medical, 2013),(D) Reynders silicone stent (Noppen, 1999), (E) Dynamic silicone stent (Rafanan, 2000) and (F) Polyflex silicone stent (Theodore, 2009) .
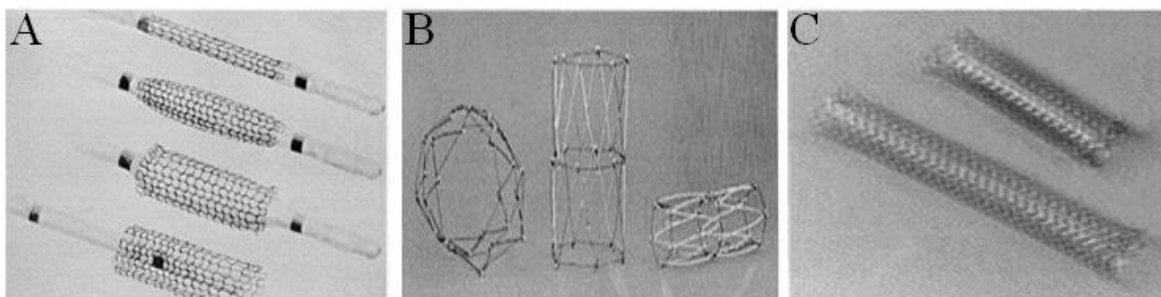
Figure 2 Metallic Stents (Rafanan, 2000). (A) Strecker balloon stent at different stages of deployment, (B) Gianturco-Z self-expanding stent, (C) covered and uncovered wallstent.

Metal stents are generally placed in a collapsed position and then expanded to achieve as much of a custom fit as possible (Zakaluzny, 2003). In comparison, silicone stents are usually folded and released in place to expand to their preformed shape. Thus, the metal stent is firmly seated and its silicone counterpart is only as well positioned as its predetermined diameter and length allows (Zakaluzny, 2003). There is less migration with longer metallic stents compared with silicone stents or short metallic stents (Saito, 2005).

Granulation tissue formation is a common complication that is prone to the proximal and distal ends of the stent. Excessive granulation tissue can lead to obstruction of the airway (trachea) (Saito, 2005). Granulation tissue formation may be mild enough to remain asymptomatic, moderate enough to produce stridor and severe enough to lead to life-threatening respiratory distress (Zakaluzny, 2003). Complications with granulation tissue are more common with metallic stents than those made of silicone. Similar to migration, the reasons for more granulation tissue formation are inherent to the properties of the metallic stent. The rigidity of metal stents cause more irritation in the airway, the edges of metal stents place circumferential pressure on the tissue and subsequently lead to the formation of granulation tissue. In addition to causing airway obstruction, granulation tissue can become a medium for bacterial growth (Zakaluzny, 2003).

Inhibition of mucociliary mechanisms that clear the airway of secretion is another complication resulting from the use of airway stents. The mesh design of metallic stents helps to preserve mucociliary function (Chin, 2008). Unlike their silicone counterparts, metal stents permit mucosalization—integration with the tracheal wall—through their interstices thereby allowing adequate mucociliary clearance (Zakaluzny, 2003). Silicone stents, because of their solid construction inhibits mucociliary clearance. Granulation tissue also has the capacity to

impair mucociliary clearance. Lack of mucociliary clearance can lead to airway obstruction and infection.

In some instances patients are unable to tolerate stenting for long periods of time. In general, still, longer stents are not as well tolerated as short, flexible, compliant stents. Studies have shown that granulation complications are associated with tracheal stent placement (Koi, 2009). Most of the complications occur in the laryngeal region and can be prevented by avoiding stenting over the subglottic region (Ko, 2009).

Complications of placing and removing stents are common occurrences. At times the complication may be that the stent is simply unable to be placed. Stent placement may become difficult due to inherent airway disease, poor stent choice, inadequate stent sizing or lack of specific instrumentation (Zakaluzny, 2003).When patients experience complications from the metallic stents that cause airway injury or obstruction it may become necessary to remove the stent (Lunn, 2005). Complications associated with removal of stents are much more common. Stent epithelialization in conjunction with granulation tissue formation around metal stents can make their removal very difficult or nearly impossible in some cases (Zakaluzny, 2003). Given that metal stents typically become mucosalized within one month of placement they are regarded as permanent fixtures. If stent removal is necessary, they may have to be deconstructed and removed piece by piece (Zakaluzny, 2003). Removal of metallic airway stents is also associated with significant complications, health-care resources use and costs (Alazemi, 2010).

The ideal stent will combine the advantages of silicone and metallic stents. Silicone stents tend to disturb airway mucociliary clearance and migrate. Metallic stents on the other hand are semi permanent fixtures and should not be used in children because they will not grow as the child grows (Saito, 2005). They also cannot degrade spontaneously and a second surgical

procedure is needed to remove the metal stent from the body (Xin, 2008). Repeated surgery increases the cost as well as patient morbidity. In this respect biodegradable Mg based alloys could be a potential solution. Hence, proceeding with research to characterize, model and produce biodegradable options for airway stents may provide definite alternatives to surgical intervention for both malignant and benign airway stenosis in the future.

2.3 Magnesium Biocompatibility

Magnesium (Mg) biocompatibility is a key factor in this study. Mg and its alloys have been investigated as early as 1878 for their potential use as a biomaterial (Kirkland, 2012). It's present in high concentrations in sea water and is the eighth most abundant element on Earth. Mg also has excellent specific strength and low density (Alvarez-Lopez, 2010). It is the fourth most abundant cation in the human body and is largely found in bone tissue as its presence is beneficial to bone strength and growth (Purnama, 2010). Mg is vital to metabolic processes, a co-factor in many enzymes, stabilizes the structure of DNA and RNA and a key component of ribosomal machinery that translates the genetic information encoded by mRNA into polypeptide structures (Xin, 2011). Mg deficiency is reported to cause cell membrane dysfunction, an increased incidence of cancer, heart disease and susceptibility to oxidative stress. On the other hand, excess magnesium can lead to muscular paralysis, hypotension, respiratory distress and cardiac arrest; all found to be unlikely because of efficient filtration by the kidneys. *In vitro* and *in vivo* studies have shown that Mg alloys possess good biocompatibility. Mg and its alloys have been used in applications such as bone implants because their density is similar to natural bone and more adequate mechanical properties (Alvarez-Lopez, 2010). There are studies that have shown that dissolved Mg ion may promote cell attachment and tissue growth on implants (Xin, 2008).

There are many actions of Mg that are potentially relevant to airway disease; the most obvious is the relaxation of smooth muscle. Gilbert et al. performed studies with vascular smooth muscle that showed this effect is dose dependent and mediated by competition with calcium entry through voltage and receptor operated channels on the cell membrane and by inhibition of intracellular calcium release from the sarcoplasmic reticulum (Gilbert, 1992). Magnesium has been shown to cause dose-related relaxation and inhibition of contraction induced by histamine, electrical field stimulation and cholinergic agonists in airway smooth muscle tissue (Britton, 1994). This effect is mediated by calcium antagonism that may result in bronchodilation and reduction in the reactivity of the airway to inhaled bronchoconstrictor agents. These effects are likely to be complemented, by other actions of magnesium that cause bronchodilation and reduction in airway reactivity through indirect effects on airway smooth muscle via inhibition of cholinergic transmissions promotion of nitric oxide (NO) release, or through a reduction in airway inflammation through effects on prostacyclin production and mast cell and T-lymphocyte stabilization (Britton, 1994). High magnesium intake is associated with a decrease in the relative odds of airway hyper-reactivity, independent of generally recognized confounding factors, and of the major determinants of hyper-reactivity (Britton, 1994). Magnesium may have an independent effect which renders the airway less responsive to an inhaled bronchoconstrictor stimulus (Gilbert, 1992). It is therefore possible that differences in the availability of magnesium may result in differences in both airway reactivity and lung function.

Unfortunately the only limitation concerning Mg based biomaterials is their low corrosion resistance (Purnama, 2010). It has been reported that cyclic stresses (fatigue) related mechanisms are responsible for mechanical failures of implantable metallic components (Antunes, 2012). Metallic implants, like Mg based biometals, owe their resistance to the

formation of a stable, compact and continuous oxide surface film called passive film that prevents the underlying bare metal surface from coming into contact with theses aggressive ions (Antunes, 2012). However, the passive film can be locally dissolved generating pits that rapidly propagate leading to pitting corrosion. This corrosion can lead to critical fractures in a process called corrosion fatigue where there is failure of a material under the simultaneous action of cyclic loads and chemical attack (Antunes, 2012). Fast degradation rates have also been considered a result of products in the physiological environment such as phosphates, chlorides, carbonates and sulfates (Xin, 2008). Also, hydrogen gas evolves during *in vitro* and *in vivo* degradation of Mg biometals. If degradation is too fast, hydrogen may accumulate as subcutaneous gas bubbles (Antunes, 2012) and not allow the body the amount of time necessary to regulate the gas created. Nevertheless, Mg based biometals produce mainly soluble and non-toxic products.

Controlling the corrosion rate of Mg based biomaterials is of paramount importance. Work to enhance corrosion resistance has been done such as coatings with dicalcium phosphate dehydrate (DCPD), alkali heat treatments and alloying. Past alloying elements included aluminum (Al), manganese (Mn), zirconium (Zr) and rare earth (RE) metals because of their largely positive effect on the corrosion resistance of magnesium. Conversely, studies have shown that MgAl and MgRE systems should not be used because they cause harmful effects on osteoblasts as well as cytotoxicity on different cell lines and may even cause the onset of Alzheimer's disease (Witte, 2008). Aluminum can bind to inorganic phosphate causing a lack of phosphate in the body leading to dementia (Lucey, 1977). Zirconium is closely associated with liver, lung, breast and nasopharyngeal cancers (Song, 2007). Even manganese has been proven to cause neurotoxicity that can lead to Parkinsonism (Crossgrove, 2004). Since, new studies have

been done with other alloying elements such as calcium (Ca) and zinc (Zn) (Antunes, 2012).

MgCa and MgZn alloys have not shown signs of cytotoxicity such as nitrosative or oxidative

stress (Li, 2008; Yuen, 2010). In this study a MgZnCa alloy was used to test its efficacy for use

in the scaffolding of tracheal airway stents. The Zn and Ca pair present in this alloy make it a

more attractive alloy because it addresses the corrosion problem that is presented by Mg

biomaterials in addition to diminishing potential cytotoxicity.

2.4 Oxidative Stress

Since oxidative stress has been implicated in vascular, cardiac and tracheal stenosis, and

cations may contribute this phenomenon, it is imperative to investigate the role of oxidant stress

(if any) in tracheal stenosis in the presence of our MgZnCa alloy. Free radicals are chemical

species that have a single unpaired electron in an outer orbit. Cell injury caused by free radicals

is an important mechanism of cell damage in may pathologic conditions (Kumar, 2010). Those

radicals derived from oxygen represent the most important class of such species generated in

living systems (Valko, 2006). When the production of reactive oxygen species (ROS) is

increased or the scavenging systems are ineffective, the result is an excess of these free radicals,

leading to oxidative stress (Kumar, 2010). Oxidative stress has been implicated in pathologic

processes including cell injury, cancer, aging and some degenerative diseases. In the airway,

ROS and reactive nitrogen species (RNS) cause hyper-responsiveness, airway inflammation in

asthma and airway remodeling in humans and animals (Valko, 2006).

ROS and reactive nitrogen species (RNS) are generated by radiation exposure (UV light,

X-rays and gamma rays), inflammation (byproducts of neutrophils and macrophages), aging,

metal catalyzed reactions (iron, copper, chromium, cobalt, vanadium, cadmium and nickel),

endotoxic shock, byproducts of mitochondria-catalyzed electron transport reactions, present as

atmospheric pollutants and ischemia reperfusion of the heart, intestine, liver, kidney and brain (Kourie, 1998, Valko, 2006). ROS originate from both endogenous and exogenous sources. Possible endogenous sources include the electron transport system of mitochondria, cytochrome P450 metabolism, peroxisomes and inflammatory cell activation (Valko, 2006). Metabolic processes that produce ROS are the xanthine (X)/xanthine oxidase (XO) system, the cyclooxygenase pathway of the arachidonic acid metabolic system, the activated neutrophil system and the amyloid β protein system (Kourie, 1998). Exogenous sources may come from a being's environment such as air pollution or medical insertion of foreign objects among other things.

Reactive oxygen species (ROS) along with reactive nitrogen species (RNS) are well recognized for playing a dual role as being both a deleterious and beneficial species (Valko, 2006). Radicals of ROS have important roles in physiological process including cell signaling and pathogen killing as a part of the immune system (Valko, 2006). Effects of ROS include physiological role in response to noxia; ROS at low concentrations is the induction of mitogenic response. On the contrary, high concentrations of ROS can be important mediators of damage to cell structures, including lipids and membranes, proteins and nucleic acids.

Superoxide anion (O_2^-) is created through metabolic processes or post oxygen activation by physical irradiation and is considered the primary ROS. This free radical has the ability to interact with other molecules and generate "secondary" ROS either directly or universally through enzyme- or metal-catalyzed processes (valko, 2006). On the other hand, superoxide radical does not react directly with polypeptides, sugars or nucleic acids and its ability to peroxidise lipids is controversial (Valko, 2006). Superoxide is inactivated by conversion to H_2O_2 and O_2 by Superoxide dismutase (SOD) in a dismutation reaction. The hydroxyl radical (^-OH) is

highly reactive with a half-life of 1 ns forcing it to react close to its site of formation. Hydrolysis of H_2O caused by ionizing radiation produces ^-OH. In addition, production of ^-OH near DNA can cause this radical to react with DNA bases or the deoxyribosyl backbone of DNA to produced damaged bases or strand breaks. The hydroxyl radical is neutralized via conversion to water by glutathione peroxidase. Singlet Oxygen ($^1O_2$) is the metastable excited site of triplet molecular oxygen, where which all electrons are paired. It has been suggested that singlet oxygen is formed from the superoxide radical in the course of pyrimidine nucleotide oxidation. Singlet Oxygen is an important chemical and biological agent as it is involved in numerous chemical and biological processes (Weishaupt, 1976). Biologically, in the area of photodynamic reactions that involve modification or destruction of biological molecules and systems under the same oxidative conditions in many instances may also proceed via singlet oxygen pathways (Weishaupt, 1976). Singlet oxygen has been implicated in biological systems such as xanthine oxidase, linoleate-lipooxidase and NADPH-dependent microsome lipid peroxidation. Carotenoids are well established as singlet oxygen quenchers. Still, in complex biological systems, carotenoid protection alone may be insufficient (Weishaupt, 1976). Hydrogen Peroxide (H_2O_2) is generated by the enzyme SOD or directly by oxidases in intracellular peroxisomes. Hydrogen peroxide is considered a ROS because it readily reacts with biological material such as DNA, lipids and proteins (Waterman, 2008). H_2O_2 can be readily be converted to ^-OH or OCl^- (hypochlorite), which destroy microbes and cells. These ROS can act distantly from the site of activation (Kumar, 2010). SOD enzymes work in conjunction with H_2O_2 removing enzymes such as catalases and glutathione peroxidase (Valko, 2006).

Reactive nitrogen species (RNS), in biological systems, are founded primarily by nitric oxide (NO). Reactions of NO ultimately lead to the oxidation, nitration (addition of NO2),

nitrosation (addition of NO), nitrosylation of most classes of biomolecules (Patel, 1999). NO has

a dual functionality in oxidative stress where it a pro- and anti-inflammatory mediator. RNS are

formed via enzymatic oxidation of L-arginine into NO by nitrogen oxide synthases (NOS)

(Valko, 2006). Inducible nitric oxide synthase (iNOS) is one of three isoforms found in

mammalian systems and is the only inducible form. Quantitation of the changes in iNOS may

indirectly reflect NO levels. Nuclear Factor-kappa B (NF-κB) regulates inflammatory cytokines

such as tumor necrosis factor alpha (TNF-α), interleukin-1 beta (IL-1β) and interferon gamma

(IFN-γ), all of which induce iNOS expression (Murphy, 1999). Nitric oxide produced by iNOS

can contribute to the cell death that may occur, however, necrosis is thwarted when free radicals

are rapidly removed.

   To balance the harmful effects of ROS antioxidants take action. These antioxidants are

non-enzymatic antioxidants that work in conjunction with antioxidant enzymes to bind to free

radicals and hinder them from interactions with lipids proteins or DNA molecules (Valko, 2006).

Important antioxidants in this study include superoxide dismutase (SOD) and glutathione S

transferase (GST), a vital enzyme that contains a "family" of nine enzymes that aide in

detoxification. These enzymes speed up the linking of toxic compounds to the "master"

antioxidant glutathione (GSH). Super oxide dismutase works by dismuating the superoxide anion

to H_2O_2 and O_2.

2.5 Hypothesis and Objectives

   At this time, the specific effect of a magnesium zinc calcium alloy on tracheal epithelia is

unknown. Currently, degradable magnesium alloys are being held as promising biomaterials for

applications in orthopedic and trauma surgery (Zhang, 2010). Research suggests that magnesium

oxide (MgO), in the form of nanoparticles, are soluble in the epithelial lining fluid of the lungs

that reduces irritation and health effects consequences (Feng, 2011). Magnesium alloys containing calcium polyphosphate particles have been found to have good mechanical properties and controlled degradation (Feng, 2011). Additionally, Mg did not inhibit cell growth and enhanced bone cell adhesion (Staiger, 2006). A recent study conducted in our lab demonstrated that pure Mg was reabsorbed quickly during a 24hr exposure to normal human bronchial epithelium *in vitro* (Waterman, 2012). The inherently corrosive nature of Mg may be overcome via alloying elements. Preliminary data suggests resorbable magnesium-based materials can be utilized for the development of tracheal stents and thus, is an impetus for initiating the present study. **Therefore, we hypothesize that exposure to MgZnCa alloy will not elicit inflammation or toxicity in normal human bronchial epithelial (NHBE) cells *in vitro*.** We know that high purity mg corrodes rapidly, so most importantly we need to determine the interactions with the airway where the stent will be placed. Also, the effect of Mg alloys on NHBE cells is unknown. as a result, we want to know if Mg alloys will elicit an inflammatory or toxic response in NHBE cells.

The objectives were to:

1. Evaluate markers of cytotoxicity and functional genomics of inflammatory mediators following Mg alloy exposure.

2. Evaluate mucus production, secretion and wire morphology following Mg alloy exposure.

3. Evaluate wound healing and cell migration of NHBE cells exposed to Mg alloys *in vitro*.

CHAPTER 3

Methodology

3.1 Magnesium Samples

Magnesium zinc calcium alloy wires (0.5cm in length) were engineered in the National Science Foundation Engineering Research Center for Revolutionalizing Metallic Biomaterials (ERC-RMB) at North Carolina Agricultural and Technical State University. Pure magnesium (γ-irradiated) samples were a kind gift of Dr. Gilbert (Vice President of Research & Development, ACell Inc.).

3.2 Chemicals and Reagents

Normal human bronchial epithelial (NHBE) cells, bronchial epithelial cell basal media (BEBM), SingleQuot supplement kits, DMEM and collagen were purchased from Mediatech (Manassas, VA). Acetic acid was purchased from Sigma Aldrich (St. Louis, Missouri). TGX gels, nitrocellulose membranes and Western blot reagents were acquired from Bio-Rad (Hercules, California). Lactate dehydrogenase kits were purchased from Roche (Indianapolis, Indiana). Anti-Phospho-IκB, anti-COX-2, and anti-iNOS and anti-rabbit IgG antibodies were purchased from Cell Signaling Technology (Beverly, Massachusetts). Anti-β-actin antibody was purchased from Santa Cruz Biotechnology (Santa Cruz, California). Enhanced chemiluminescence (ECL) kits for Western blotting were purchased from GE Healthcare Life Sciences Division (Fairfield, Connecticut).

3.3 Cell Culture and Exposure

Primary normal human bronchial epithelial cells (NHBE) (CC-2540) were purchased mycoplasma free and source verified. NHBE cells were expanded for a period of 7-10

days in flasks until 70-80% confluency in high EGF BEBM expansion media containing 0.13 mg/ml of bovine pituitary extract (BPE), 0.5 µg/ml of hydrocortisone, 12.5 ng/ml of recombinant human epithelial growth factor (rhEGF), 0.5 µg/ml of epinephrine, 10µg/ml of transferrin, 5 µg/ml of insulin, 50nM of retinoic acid, 6.5 ng/ml of triiodothyronine, and 50 µg/ml of GA-1000. Confluent cultures were then trypsinized, spun down, pelleted, and cryopreserved in the vapor phase of liquid nitrogen at a density of $1x10^6$. Since recent studies have shown that magnesium ions produced by the interaction of cells with magnesium materials have caused serious problems when using cellular metabolism based assays such as MTT and LDH, we used the air liquid interface which includes trans-wells. For initial seeding, trans-well inserts contained in six-well plates were coated with collagen solution consisting of 13µg of collagen per ml of acetic acid for 1hr. Plates were then washed with 1x phosphate buffered saline (PBS) for 10 minutes. After aspiration of PBS, adherent cells were seeded onto collagen coated trans-well inserts and fed every two days for a period of 7 days with 2ml of bronchial epithelial cell basal growth medium (BEBM) supplemented with 0.13 mg/ml of bovine pituitary extract (BPE), 0.5 µg/ml of hydrocortisone, 5 ng/ml of recombinant human epithelial growth factor (rhEGF), 0.5µg/ml of epinephrine, 10 µg/ml of transferrin, 5 µg/ml of insulin, 50nM of retinoic acid, 6.5 ng/ml of triiodothyronine, and 50 µg/ml of GA-1000. After 7 days, cells were taken to air liquid interface by aspirating media off the apical surface of the NHBE cell monolayer. Cells were then fed daily with 2ml of BEBM growth media for 14days and until mucus layer was present. Magnesium wires were manually placed on the apical surface of the cell/mucus monolayer for a time period of (0-48hrs). Microscopic observation was obtained 0hr, 4hr, 18hr, 24hr, and 48hrs using an EVOS digital inverted light microscope (Advanced Microscopy Group, Bothell, Washington).
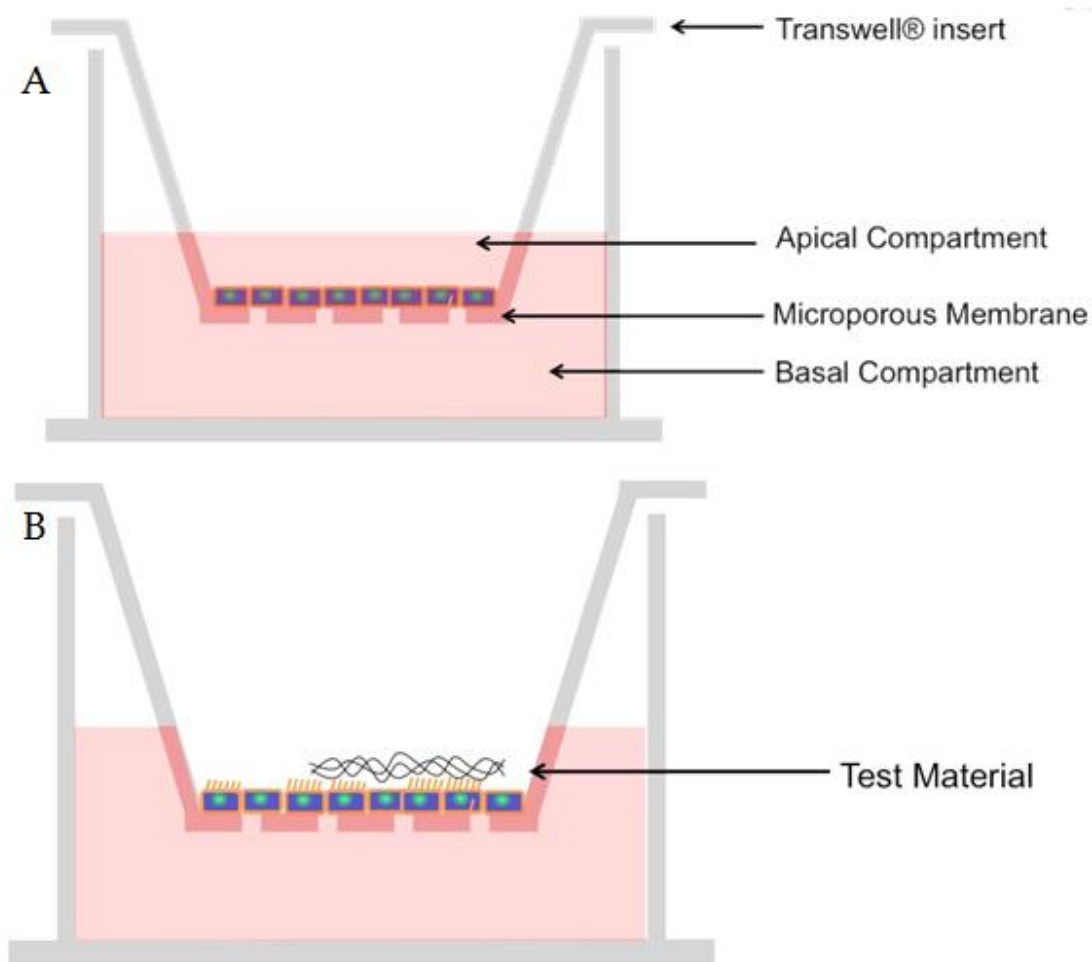
Figure 3 Schematic of the air liquid interface. An air liquid interface (A), displaying the transwell insert, apical compartment, microporous membrane (where cells rest) and basal compartment. (B) Fully differentiated NHBE cells exposed to the test material at the apical surface (Image developed by Dr. Thomas Gilbert).

3.4 Lactate Dehydrogenase Assay (LDH)- Cytotoxicity Assay

To determine the cytotoxic effect of magnesium wires on NHBE cell line, the lactate dehydrogenase assay was used by Roche. Lactate dehydrogenase (LDH) is a ubiquitous enzyme located in the cytoplasm of all mammalian cells. The release of this enzyme indicates a disruption of the plasma membrane thus a reduction in cell vitality. The spent media of NHBE

cells cultured in air-liquid interface was collected from the basal compartment after 24hr and 48hr exposure to magnesium nanowires. The low and high controls as well as experimental wells were collected and then spun down to eliminate cell contamination. The supernatant was then placed in fresh 96 well plates and LDH was detected according to manufacturer's instructions using a Molecular Devices VersaMax microplate (Sunnyvale, California) reader at 490 nm.

3.5 Reverse Transcription Polymerase Chain Reaction (RT-PCR)

Total RNA was isolated using an RNeasy mini kit and an RNase-free DNase set (Qiagen, Valencia, CA). RNA (800ng) from each treatment group and control was reversed transcribed to produce cDNA using the iScript cDNA synthesis kit (Bio-Rad, Hercules, CA) according to manufacturer's instructions. Briefly, the total RNA (800ng) was combined with 5X iScript Reaction mix, nuclease-free water and iScript Reverse Transcriptase in a 25 μl reaction. The samples were incubated in a iCycler thermal cycler (Bio-Rad) using the following reaction protocol: 5 minutes at 25°C, 30 minutes at 42°C, 5 minutes at 85°C and held at 4°C. The generated cDNA was then probed for pro-inflammatory mediators and antioxidants using the primers described in Table 1. produced from Invitrogen software. For the amplification of cDNA, GoTaq® Green Mastermix (Promega, Madison, WI) and protocol were used according to manufacturer's instructions. For a 25ul reaction, 12.5μl of 2x GoTaq® Green Mastermix, 1μl of forward primer, 1μl of reverse primer, 4μl of template DNA, and 6.5μl of nuclease free water were combined and added to a RNase free and sterile PCR plate for each gene and sample. The samples were incubated in a preheated (95°C) iCycler thermal cycler (Bio-Rad) using the following reaction protocol: 4 minutes at 94°C; 35 cycles of 95°C for 30 seconds, 60°C for 30 seconds, 72°C for 1 minute; and post-extension for 4 minutes at 72°C; and hold at 4°C. PCR products were resolved on 1% agarose gel in 1X Tris-Borate-EDTA buffer , pH 8.0 (Boston

Biologicals, Wellesley, MA) at 160 volts (V) and visualized using ethidium bromide. All values were normalized to the constitutive expression of the housekeeping gene, β-actin.

Table 1

Primers Used in Polymerase Chain Reaction.

Primers	Oligonucleotide Sequence 5'→ 3'	Tm (°C)	Amplicon Length (bp)
H_Bactin-Fwd	ATGGATGATGATATCGCCGCG	57.5	
H_Bactin-Rev	CTAGAAGCATTTGCGGTGGGAC	58.4	113
H_NFκB-Fwd	CACCTAGCTGCCAAAGAAGG	60.0	
H_NFκB-Rev	GCCAATGAGATGTTGTCGTG	60.0	657
H_NOS-2-Fwd	ACAAGCCTACCCCTCCAGAT	60.0	
H_NOS-2-Rev	TCCCGTCAGTTGGTAGGTTC	60.0	717
H_GST-1-Fwd	AGAAGGTGTGGCAGATTTGG	60.0	
H_GST-1-Rev	CTTCAGCAGAGGGAAGTTGG	60.0	645
H_SOD-2-Fwd	GGAACGGGGACACTTACAAA	60.0	
H_SOD-2-Rev	TCTTGCTGGGATCATTAGGG	60.0	750

3.6 Western Blot Analysis

Whole cell lysates were extracted from NHBE cells in control and magnesium wire exposed groups and quantitated using the Bradford assay. Equal amounts of protein were loaded in each lane with 4x sample loading buffer. Samples were boiled at 100 °C for 5 min before gel loading. Lysates (50μg) were then fractionated using 10% TGX gels (Bio-Rad) by sodium

dodecyl sulfate-polyacrylamide gel electrophoresis (SDS-PAGE) at 150 volts for 45 minutes. Fractionated proteins were transferred to nitrocellulose membranes using a semi-dry method at 10V for 60 minutes. After blocking in 5% milk, nitrocellulose membranes were washed twice with tris-buffered saline-tween (TBS-T). Membranes were probed with primary antibody in 5.0% bovine serum albumin solution (BSA) and gently rocked overnight at 4°C. Primary antibodies used were anti-human rabbit Phospho-IκB (Cell Signaling), anti-human rabbit, anti-human rabbit SOD-1 (Cell Signaling), anti-human rabbit GST (Cell Signaling), anti-human rabbit iNOS (Cell Signaling) and goat β-actin (Santa Cruz) at a concentration of 1:1000. Probed membranes were washed and secondary antibody anti-rabbit IgG (Cell Signaling) (1:2000) were used to detect primary antibodies. After washing, ECL detection reagents will be added (3ml) to probed membranes for one minute and subsequently imaged using Bio-Rad imaging technology; band densities will be analyzed using image lab (Bio-Rad).

3.7 Mucin Enzyme Linked Immunosorbent Assay (ELISA)

To examine the effect of Mg and magnesium alloy wires on mucin production, an in-house enzyme linked immunosorbent (ELISA) assay was used. Magnesium and Mg alloy nanowires were placed in the cell/mucus monolayer for 24hrs. After exposure, NHBE cells were then rinsed with 500 µl of 1x PBS containing 100 µM dithiothreitol (DTT) followed by a second rinse of 500 µl of 1x PBS. Each rinse was collected and pooled for mucin ELISA analysis. β-mercaptoethanol (12.5M/5µl) was added to each sample for a final concentration of 50mM and mixed well. Mucin samples were then centrifuged at 8,000rpm for 5 minutes. Dilutions of each sample (1:10, 1:30 and 1:50) were made in triplicate using 1x PBS, pH 7.4 and added to 96 well plate. Undiluted standards in duplicate were also added and incubated at room temperature for 2hrs and then overnight at 4°C. After incubation, contents of each well were discarded and

washed twice with 1xPBS, pH 7.4. Blocking solution (200µl) containing 3% bovine serum albumin in 1x PBS, pH 7.4 was added to each well and incubated at room temperature for 2hrs. Wells were then washed twice with 1x PBS, pH 7.4. Primary antibody was diluted (1:1000/50µl) in 0.3% BSA/PBS, pH 7.4 was added to the entire 96-well plate and incubated at room temperature for 1hr. Subsequently, wells were washed three times with 1x PBS, pH 7.4 and probed with 50µl of secondary antibody, anti-human IgG-HRP linked (1:2000)(Santa Cruz) and incubated at room temperature for 1hr. Well contents were discarded and washed five times with PBS, pH 7.4. For detection, a 1:1 dilution of TMB substrate solution (KPL, catalog#50-76-02) and TMB peroxidase solution (KPL, catalog#50-65-02) were added to each well (50 µl) and incubated for 30 minutes. Following addition of 50 µl of stop solution (1M H_2SO_4), absorbance was read at 450 nm using a VersaMax microplate reader (Molecular Devices).

3.8 Scanning Electron Microscopy (SEM)

After incubation with NHBE cells in air liquid interface for 24hrs or 48hrs, magnesium alloy wires were collected and examined by SEM to characterize the surface morphology of the recovered wires. A Hitachi SU8000 Field Emission Scanning Electron Microscope (SEM) was used to capture images on the micro- and nano-scale. Each sample was placed on a stage and attached using copper tape. Once the stage was prepared, it was inserted into the chamber which creates a vacuum seal before the specimen enters the microscope. During microscopic visualization, a low magnification setting was used to capture images of the specimen. Voltages from 1-20 kV were used to obtain the acceptable pictures of pure Mg and MgZnCa alloy wires. Brightness, contrast, and alignments were adjusted as needed.

3.9 Wound Healing Assay

Cellular interaction and migration potential in response to magnesium alloy wires was evaluated by utilizing the wound repair method. After 21days, the NHBE cell monolayer, including mucus layer, will be cut 2-3 cm using a sterile blade. One magnesium alloy wire will be inserted into the wound for a period of 24hrs and 48hrs. Phase contrast microscopy images were taken at 0hr, 4hrs, 18hrs, 24hrs, and 48hrs with the EVOS microscope, to monitor the progression of wound healing and cellular migration.

3.10 Statistical Analysis

Statistical differences between the means were determined with a one-way analysis of variance (ANOVA) software and a treatment effect with P values less than 0.05 considered significant. All experiments were performed in triplicate and three biological replicates were completed. Results were expressed as means of $\pm$ standard deviation of at least three biological experiments. Individual groups were compared with the unpaired Bonferroni post-test corrections.

CHAPTER 4

Results

4.1 Evaluation of the Expression of Inflammatory Mediators at the Gene and Protein levels and Cytotoxicity.

The evaluation of gene modulation is a necessary assessment that gives insight of molecular changes induced by cellular interaction with biomaterial substrates. Genomic profiles of NHBE cells exposed to magnesium alloy wires for 24hrs were obtained for NFκB, iNOS, SOD and GST via a polymerase chain reaction. In Figure 4, there are no differences between the control (cells only) value and MgZnCa alloy expression of pro-inflammatory mediators; NFκB, fig. 4A and iNOS fig. 4B or antioxidants GST, fig.4C and SOD, fig. 4D. No inflammatory processes were up-regulated due to the presence of magnesium alloy biomaterials.
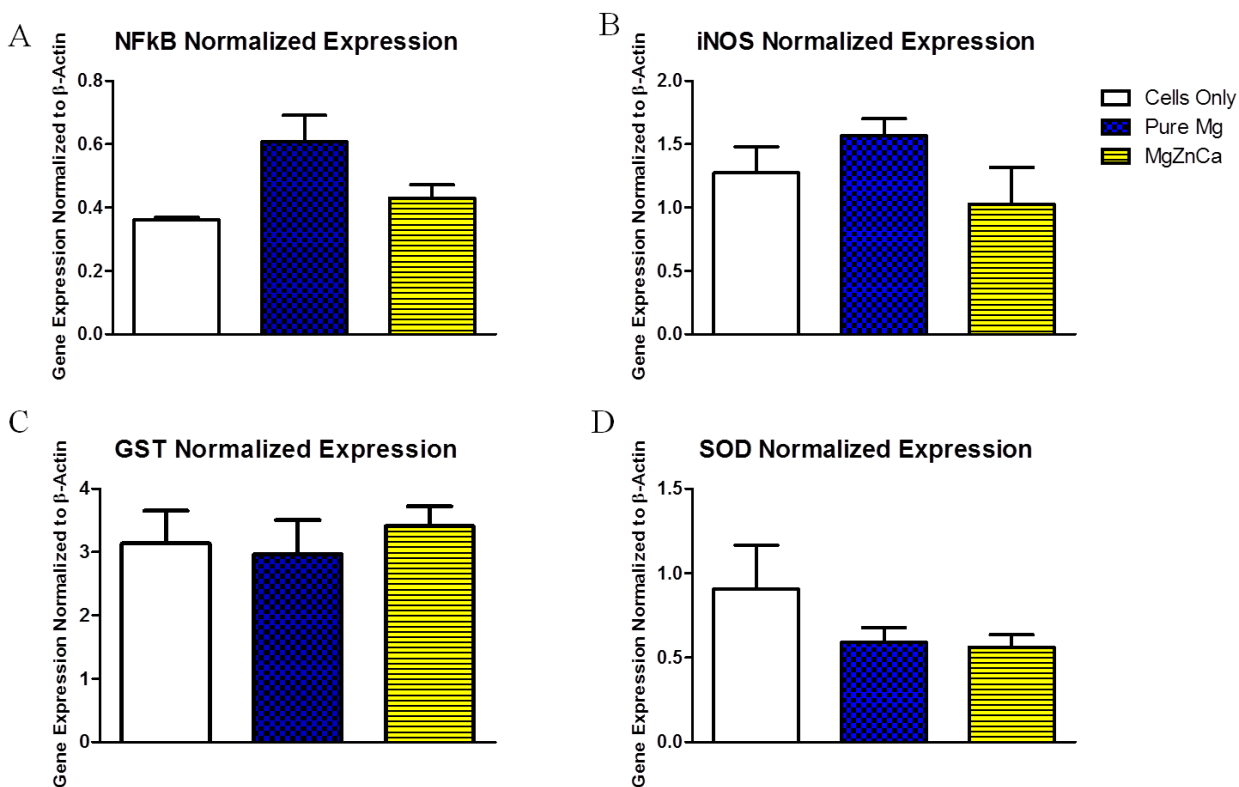
Figure 4 Gene expression of pro-inflammatory mediators and antioxidants. Quantitative polymerase chain reaction reveals no significant modulation (P value > 0.05) of transcription factor NF-κb(A), pro-inflammatory mediator iNOS (B) or antioxidants SOD (C), and GST (D), in NHBE cells after 24hr exposure to magnesium wires Data represents the mean ± SEM, n=3.

4.1.1 Modulation of Pro-inflammatory and antioxidant proteins in response to Mg Alloy Wire Exposure. Using the Western blot method to validate genomic profiles of NHBE cells exposed to magnesium alloy wire for 24hr, P-IκB-α (fig. 5A and fig. 6A), a regulator of NFκB, was found to have little to no expression in the presence of the MgZnCa alloy. The phosphorylation and degradation of IκB-α symbolizes the inactivation of the inhibitory complex composed of IκB-β and IκB-α. This complex prevents NFκB, which is normally sequestered in the cytoplasm, from entering into the nucleus and transcribing pro-inflammatory genes such as inducible nitric oxide or iNOS (fig. 5B and fig. 6B). We found that there was no appreciable phosphorylation of IκB-α suggesting that the presence of the magnesium alloy for 24hrs did not induce NF-κB-regulated oxidative stress compared to the unexposed cells. In similar studies, the generation of free radicals *i.e.,* oxidative stress from the presence of metal alloys, were found to induce the phosphorylation of IκB encouraging the transcription of key pro-inflammatory proteins (Valko, 2006). Antioxidants superoxide dismutase, fig. 5C and fig. 6C, and glutathione-s-transferase were not depleted in the presence of the MgZnCa alloy.
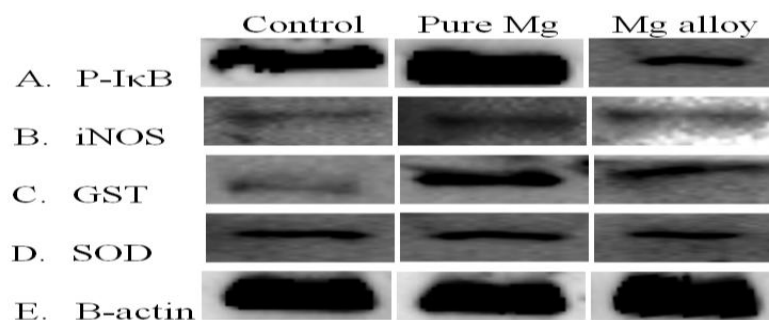
Figure 5 Expression of pro-inflammatory and antioxidant proteins. Immunoassay of phosphorylated inhibitor of kappa B alpha, P-IκBα (A), Inducible Nitric Oxide Synthase, iNOS (B), Glutathione-S-Transferase, GST (C), and Superoxide Dismutase, SOD (D), revealed that there was no detectable inflammation caused by a 24hr exposure to wires of Mg or Mg alloy. Beta-actin (E), expression was used as loading control. Bands show are representative of six blots.
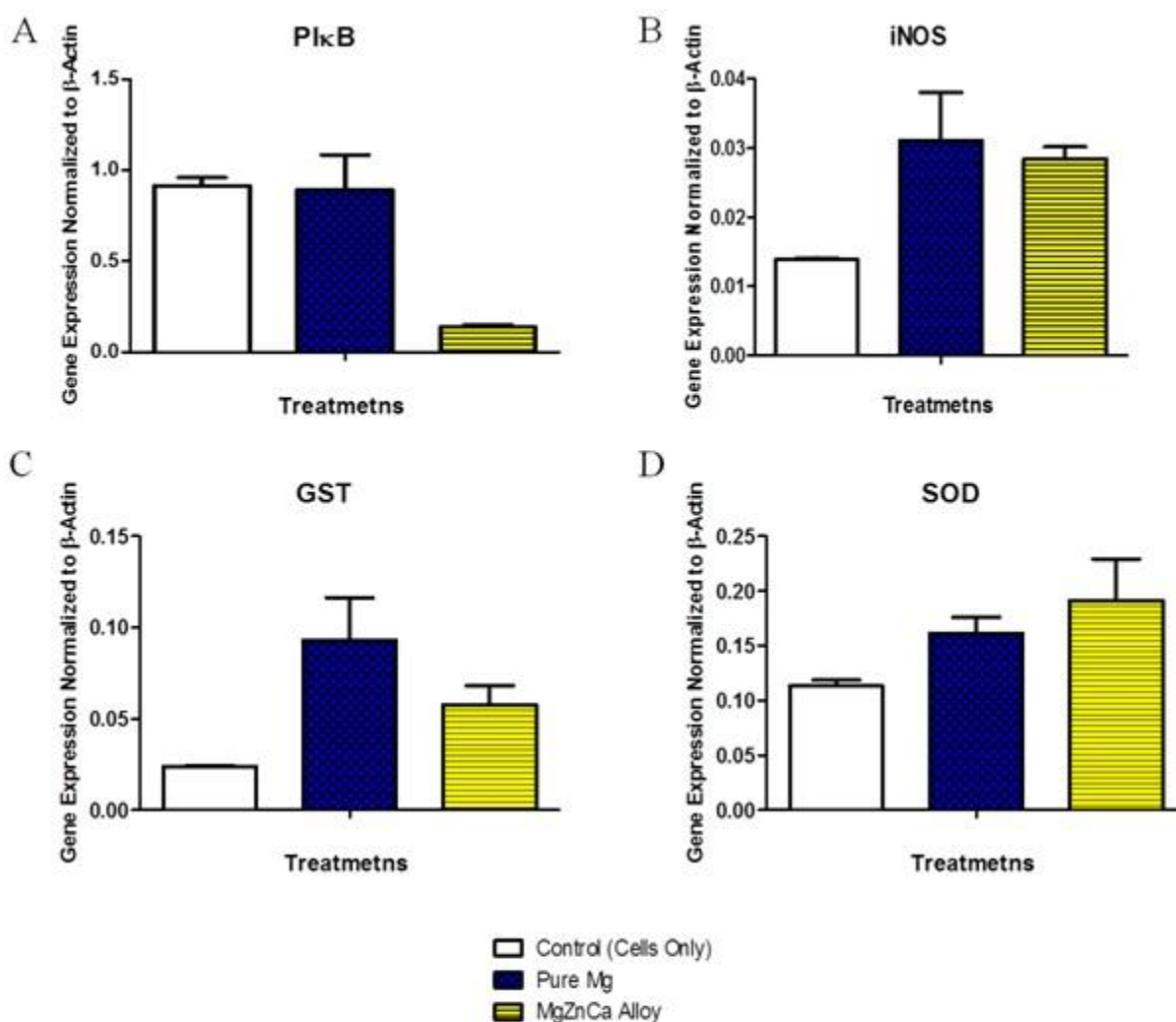
Figure 6 Protein expression of pro-inflammatory mediators and antioxidants. Densitometric analysis of P-IκBα (A), iNOS (B), GST (C), and SOD (D), protein expression in NHBE cells after 24hr exposure to Mg wires shown in figure 5. There was a significant difference in the expression of P-IκBα between the Pure Mg and our Mg alloy (P value < 0.05). No differences between iNOS, GST and SOD protein expression levels as determined by one-way analysis of variance (ANOVA) (P value > 0.05). Data represents the mean $\pm$ SEM, n=6.

4.1.2 Cytotoxicity. In recent studies, magnesium ions produced by the interaction of cells with magnesium materials have caused serious problems when using cellular metabolism based assays such as MTT and LDH; false negatives or positives and interference with dye stability have been an issue when analyzing the biocompatibility of metal alloys *in vitro* (Witte, 2008). In these studies the magnesium metal came in direct contact with the media that was in turn tested for cytotoxicity. However, within this study, our experimental design, which employs use of the unique air liquid interface cell culture model, provides layers of separation between wires and cell culture media and prevented Mg ion interference; the media collected for the LDH measurement was collected from the basal compartment (see figure 3). The activity of LDH was monitored at 24hr and 48hrs for control and Mg alloy wires exposed NHBE cells. Magnesium wire only controls were also incorporated. Fig.7 shows at our time points of interest (24hrs and 48hrs) there was little to no cytotoxicity. It should be noted that fully differentiated NHBE cells demonstrate high levels of lactate dehydrogenase release, thus levels in control cells are normally high. We feel that the presence of the high purity Mg and Mg alloy wires aide in cell viability. At the time points of interest, the LDH levels decrease with Exposure to Mg and Mg alloy wires.

Figure 7 Lactate dehydrogenase evaluation. Lactate dehydrogenase assessment to determine plasma membrane damage of NHBE cells in air-liquid interface exposed to magnesium wires for 24hr and 48hr. Data are presented as mean ± SEM; n=3.

4.2 Evaluation of Mucin Production and Secretion following Mg Alloy Exposure *in vitro*.

Mucus lubricates the airways and helps in the removal of foreign particles that might have been inhaled, such as dust or bacteria (Ji, 1999). The airways are normally cleared of excess mucus and foreign particles by a combination of coughing and mucociliary clearance, which is the coordinated movement of tiny hairs (cilia) that project into the mucus-lined airways (Kumar, 2010). Additional mucus is produced during infection or when there is airway irritation, from smoke or dust, for example (Reed, 2001). Hypersecretion from hyperplastic goblet cells causes airway mucous plugging, especially in peripheral airways, where large, numerous secreting goblet cells can more easily cause obstruction (Reed, 2001). An enzyme linked immunosorbent assay (ELISA) was utilized to determine if magnesium and magnesium alloy wires inhibited or increased mucin production in NHBE cells. At 24hrs, a slight reduction in magnesium alloy wires- mediated mucin production was found in relationship to the control (Figure 8). Mucin

production and cell migration were unaffected due to magnesium alloy interaction suggesting that cell

cycle progression, cell growth and functionality were maintained.

Mucin ELISA
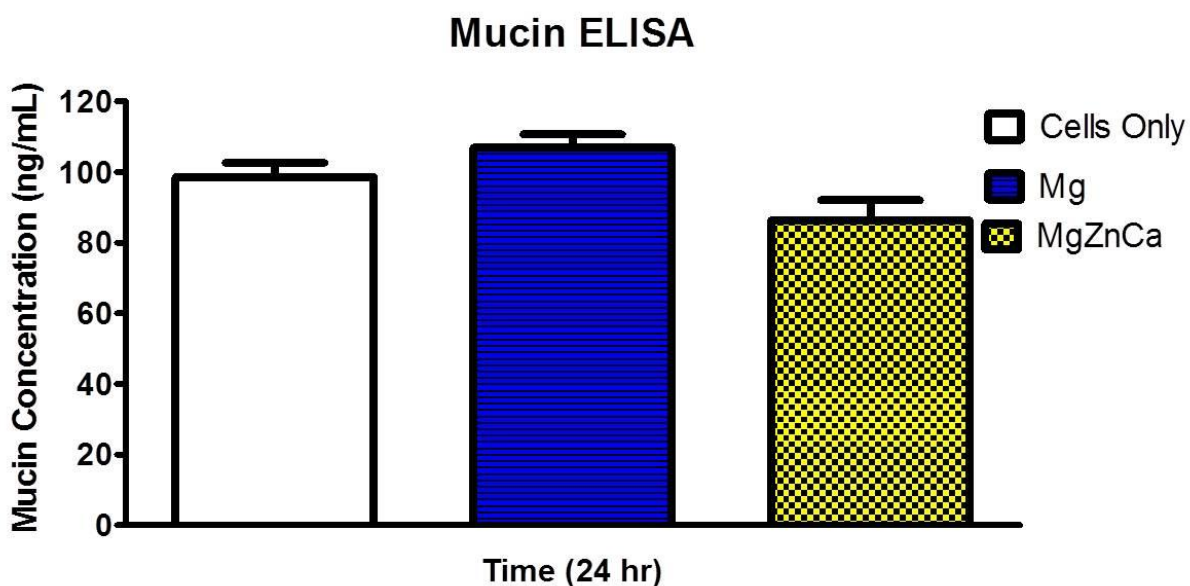
Figure 8 Airways mucus secretion assessment. *In vitro* evaluation of global mucin production in

NHBE cells, where mucin was collected following 24 hr exposure to Mg wires. Wires of Mg

caused more mucin secretion than wires of a novel MgZnCa alloy in fully differentiated human

airway epithelial cells *in vitro* (p value = 0.0253) as determined by a Pan-Mucin ELISA. Data are

presented as mean ± SEM, n=9.

4.2.1 Evaluation of cell migration of cells exposed to MgZnCa alloys and evaluate

wire morphology following exposure to MgZnCa alloys in vitro. It is known that Mg is prone

to degrade rapidly at physiological pH (7.4); therefore, it is important to monitor the degradation

the Mg alloy wires underwent after 24hrs of exposure to mucus-secreting cultures of NHBE

cells. The evaluations shown in figure 9 shows that there was minimal degradation of the

MgZnCa alloy (D-F) in comparison to pure Mg wires (A-C) which underwent mass degradation.
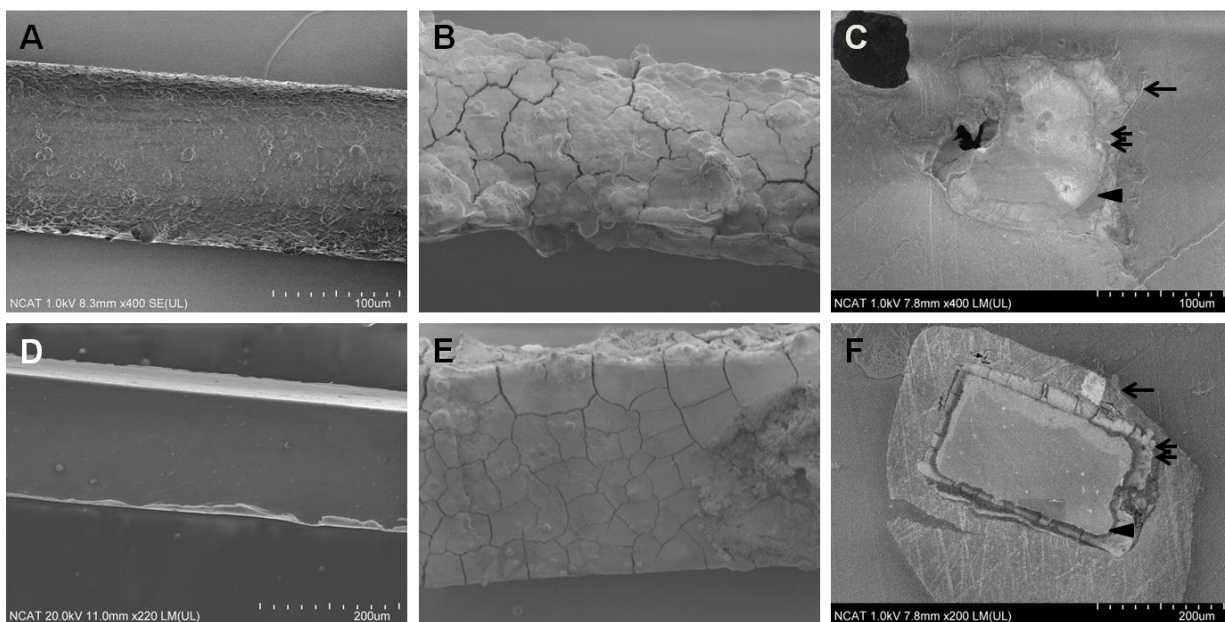
Figure 9 Scanning Electron Microscopy images of Mg and MgZnCa alloy wires. SEM imaging of wires of Mg and MgZnCa (A, D) before and (B, E) after 24hr exposure to NHBE cells *in vitro*. Cross-sections of (C) Mg and (F) MgZnCa post-exposure revealed concentric layers consisting of a mucus-based capsule (arrow) surrounding corrosion product (double arrows) atop the metal core (arrow head).

4.3.2 Wound repair. The wound repair assay has been used to evaluate the potential of various agents to close manually or chemically induced wounds for many years. It is well established that magnesium is a cofactor in many processes within the body. To determine the impact of magnesium alloys on wound repair, magnesium alloy wires were placed in a NHBE cell monolayer wound for 24hr and 48hrs. The progress of wound healing is depicted in Figure 10 was recorded at 0hr prior to injury, fig. 10A, 4hrs after injury (fig. 10B (pure Mg) and fig. 10F (MgZnCa alloy)), 18hrs post injury (fig. 10C, pure Mg and fig. 10G, MgZnCa alloy), 24hrs post injury (fig. 10D, pure Mg and fig. 10H, MgZnCa alloy) and 48hrs post injury (fig. 10E, pure Mg and fig. 10I, MgZnCa alloy). Cell migration and wound closure can be noted.
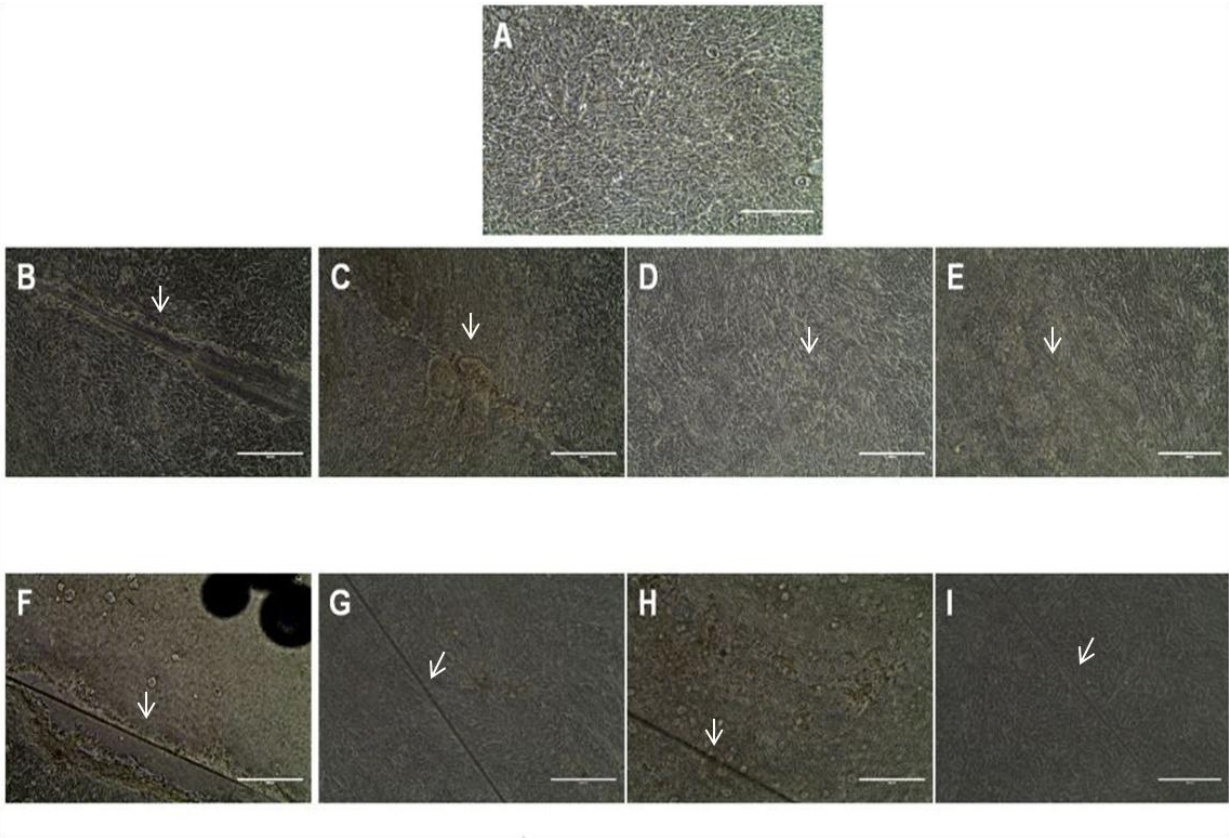
Figure 10 Wound closure in NHBE monolayer cultured with Mg-based wires. EVOS micrographs of fully differentiated NHBE monolayer prior to injury (A) and Mg (B-E) and MgZnCa (F-I) wire exposure at 4hr (B,F), 18hr (C,G), 24hr (D,H) and 48hr (E,I) time points. Note cell migration and wound closure (arrow). Data represents the mean $\pm$ SEM, n=6.

CHAPTER 5

Discussion

Treating tracheobronchial disorders caused by malignant or benign tumors, extrinsic compression, post-intubation tracheal injuries, tracheomalacia or sequelae caused after tracheostomy is a complex issue requiring a multifaceted solution. Common treatments range from balloon dilations to conventional surgical treatments and even highly invasive surgical procedures. Interventional pulmonology otherwise known as airway stenting has developed in the field of pulmonary medicine focused on using bronchoscopic techniques to treat airway disorders (Saito, 2005). Stents can be classified into silicone (or synthetic rubber) tube stents or metallic stents. Silicone stents are relatively inexpensive and easily molded to various degrees of firmness and flexibility. They have good tolerance and can be removed easily even after years of placement. Their major disadvantage is that the frequently migrate causing reocclusion. Metallic stents are slowly gaining popularity because of their ease of insertion and have greater radial force, flexibility and dynamic expansiveness (Rafanan, 2000). There is less frequent migration with metal stents because they are typically incorporated in the bronchial mucosa making them permanent. Metallic stents have been associated with formation of granulation tissue, fistula development and difficult recovery (Saito, 2005). The disadvantages of metallic stents are outweighed by their benefits. To alleviate many of these obstacles, the optimization of the stent material has been implemented.

In this study we evaluated the biocompatibility of magnesium alloy wires with fully differentiated airway epithelial cells *in vitro*. To date, there have been few studies evaluating the efficacy of magnesium alloys as a core material for tracheal stenting. It was determined that there was no appreciable modulatory effect on key pro-inflammatory genes and proteins of the NF-κB

signaling pathway. Cytotoxicity analysis of MgZnCa exposed cells yielded results correlating with genomic and proteomic analyses in that lactate dehydrogenase activity levels were not elevated after 24hr and 48hr. Mucin production and cell migration were unaffected due to magnesium alloy interaction suggesting that cell cycle progression, cell growth and functionality were maintained. Magnesium has been used in orthopedic implants and cardiovascular stenting (Purnama, 2010), and thus has high biocompatibility. However, to date, there has been little to no studies that evaluate the efficacy of using Mg based alloys as a foundation material for tracheal stenting. In this current study, a novel MgZnCa alloy showed promise as a candidate for primary use in tracheal stent scaffolding using an *in vitro* air liquid interface culture model.

The generation of metal ions from degraded metal biomaterials has been thought to promote oxidative stress (Purnama, 2010). When the production of reactive oxygen species (ROS) is increased or the scavenging mechanisms are ineffective, the result is an excess of these free radicals, leading to oxidative stress (Kumar, 2010). Oxidative stress can activate important pro-inflammatory transcription factors, mainly NF-κB. In similar studies oxidative stress arising from the presence of metal alloys, was found to induce the phosphorylation of IκB that ultimately encouraged the transcription of key pro-inflammatory proteins (Valko, 2006). Genomic and proteomic evaluation of NHBE cells, in this study, exposed to the novel MgZnCa alloy showed no significant modulation of NF-κB (or P-IκB in proteomic analysis). This is consistent with preliminary studies with pure Mg samples (Waterman, 2012). Since NF-κB complex remained sequestered in the cytoplasm, pro-inflammatory genes like iNOS was not transcribed and did not show significant modulation in this study. Antioxidants tested in this study, superoxide dismutase (SOD) and glutathione-S-transferase, also confirm the absence of oxidative stress as they were not depleted in the presence of the novel MgZnCa alloy. One study

used to assess the possible mechanism of action of chromium (VI) and arsenic (III) ions, found that NF-κB activation was inhibited through the interference of inhibitory molecule, IKK and NF-κB DNA binding or from impeding the activity of cAMP-responsive element binding protein or (CREB) (Kippler, 2012). Since NF-κB is also responsible for cell growth, cell cycle progression, and neoplastic transformation (Chen, 2002), we know that the presence of magnesium ions did not inhibit the transcriptional activity of NF-κB, because of the elevated level of cell migration seen in the wound repair assays.

The occurrence of cytotoxicity in relationship to cell/alloy interaction can be caused by many factors. One main factor is the influx of metal ions from the degradation of implanted biomaterials. Increases in systemic levels of metal alloying ions such as manganese have been found to induce neurotoxicity (Crossgrove, 2004) and zirconium ions have been found to be associated with liver, lung, breast and nasopharyngeal cancers (Song, 2007). In this study, it was determined that our MgZnCa alloy caused negligible stimulatory or deleterious effects on differentiated cultures of NHBE cells *in vitro*.

CHAPTER 6

Conclusion and Future Directions

As the journey toward developing a reliable biodegradable stent progresses, we know that there are many challenges that lie ahead. Overcoming problems with traditional stents is key to developing the ideal stent. Zakaluzny described the ideal stent as; (1) one that is easy to insert and remove, (2) has expansion force adequate to maintain airway patency against compressive without causing pressure to the mucosa that could damage the airway, (3) that is available in different sizes to accommodate various airway sizes and obstructions, (4) one that maintains its placement in the airway without migration, (5) is made of material that does not irritate the airway, (6) does not obstruct the airway tributaries and (7) does not inhibit mucociliary action (Zakaluzny, 2003). Unfortunately there is not a stent that maintains all of these qualities, however, this study provides progressive step towards creating the ideal airway stent.

In the present study, using an air liquid interface model, fully differentiated NHBE cells were exposed to a novel MgZnCa alloy and was shown to perform as well as, and at times, better than, high purity Mg. We have determined via functional genomic analysis that the novel MgZnCa alloy had no modulatory effect on pro-inflammatory transcription factor NF-κB or pro-inflammatory mediatory iNOS. There was no degree of difference in the expression of P-IκBα or iNOS proteins exhibited in our western blot analysis, subsequently validating our genomic evaluation. Antioxidants SOD and GST were not depleted in the presence of the MgZnCa alloy via genomic and proteomic confirmation. Airway cell migration and wound closure was enhanced in the presence of the novel MgZnCa alloy as confirmed by the wound repair assay. Cytotoxicity analysis also correlated with genomic and proteomic evaluations in that no appreciable increases in LDH release were found after exposure to novel MgZnCa wires for

24hrs and 48hrs. Based on SEM images, we are able to determine that MgZnCa alloys underwent less degradation and made for a more resilient alternative material compared to pure Mg. in addition, we are able to conclude that due to less degradation of the novel MgZnCa wires there was less mucin secretion compared to pure Mg confirmed via a mucin ELISA.

An obvious limitation in the present study is that a 'static' culture system where culture media was changed either a few times or once daily was utilized. An ideal *in vitro* system would by dynamic where media and air are continuously circulated to simulate respiration and blood flow, such as seen with bioreactor technologies. Currently, efforts are underway to develop a suitable bioreactor to maintain and investigate the cellular responses in the airway. Even with its obvious limitations, the ALI cell culture model used here is the current state-of-the-art for evaluating *in vitro* responses of differentiated tracheobronchial epithelial cell cultures because cells grown in this manner are essentially identical in anatomy and physiology to the same cells within the body (personal communication with Dr. Jenora Waterman) and thus, is reliable for understanding potential effects *in vivo*.

Future studies may include the incorporation of biofunctional coatings alone or together with pharmaceuticals (*e.g.*, antibiotics) with Mg alloy stent materials and evaluation of cytocompatibility. Given that metal stents can cause granulation tissue and granulation tissue can become a culture medium for bacteria. Cultures of granulation tissue have shown to grow numerous bacteria such as *Streptococcus viridians*, *Pseudomonas aeruginosa*, nonhemolytic streptococci and *Staphylococcus aureus* (Zakaluzny, 2003). Silver has been used for thousands of years as a precious metal by humans in different applications and the antimicrobial activity of silver appears significantly high. It is more toxic to microorganisms than any other metal (Ansari, 2011). Preliminary studies in our lab suggest that silver may provide antimicrobial

properties through inhibition of bacterial that dominate the airways of asthmatics (unpublished studies).

In conclusion, the work presented here support the efficacy of using the novel MgZnCa alloy in the development and manufacture of tracheal stents.

References

Adcock, I., Ford, P., Ito, K., & Barnes, P. (2006). Epigenetics and airways disease. *Respiratory Research, 7*(1), 21.

Alazemi, S., Lunn, W., Majid, A., Berkowitz, D., Michaud, G., Feller-Kopman, D., . . . Ernst, A. (2010). Outcomes, health-care resources use, and costs of endoscopic removal of metallic airway stents. *Chest, 138*(2), 350-356. doi: 10.1378/chest.09-2682

Alvarez-Lopez, M., Pereda, M. D., Del Valle, J., Fernandez-Lorenzo, M., Garcia-Alonso, M., Ruano, O., & Escudero, M. (2010). Corrosion behaviour of AZ31 magnesium alloy with different grain sizes in simulated biological fluids. *Acta Biomaterialia, 6*(5), 1763-1771.

Ansari, M. A., et al. . (2011). Evaluation of anitbacterial activity of silver nanoparticles again MSSA and MRSA on isolate form skin infections. *Biological Medicine 3.2*, 141-146.

Antunes, R. A., & de Oliveira, M. C. L. (2012). Corrosion fatigue of biomedical metallic alloys: Mechanisms and mitigation. *Acta Biomaterialia, 8*(3), 937-962.

Britton, J., Pavord, I., Richards, K., Wisniewski, A., & et al. (1994). Dietary magnesium, lung function, wheezing, and airway hyper-reactivity in a random adult population sample. *The Lancet, 344*(8919), 357-362.

Carden, K. A., Boiselle, P. M., Waltz, D. A., & Ernst, A. (2005). Tracheomalacia and Tracheobronchomalacia in Children and Adults*An In-depth Review. *CHEST Journal, 127*(3), 984-1005. doi: 10.1378/chest.127.3.984

Chen, F., and Xianglin Shi. . (2002). "Signaling from toxic metals to NF-kappaB and beyond: not just a matter of reactive oxygen species." *Environmental health perspectives, 110*(Suppl 5).

Chin, C. S., Litle, V., Yun, J., Weiser, T., & Swanson, S. J. (2008). Airway stents. [Review]. *Ann Thoracic Surgery, 85*(2), S792-796. doi: 10.1016/j.athoracsur.2007.11.051

Crossgrove, J., & Zheng, W. (2004). Manganese toxicity upon overexposure. *NMR in Biomedicine, 17*(8), 544-553.

Feng, A., & Han, Y. (2011). Mechanical and *in vitro* degradation behavior of ultrafine calcium polyphosphate reinforced magnesium-alloy composites. *Materials & Design, 32*(5), 2813-2820.

Gilbert, D. A. E., Singer, HA, Rembold CM. (1992). Magnesium relaxes arterial smooth muscle by decreasing intracellular Ca2 + without changing intracellular Mg2+. *Journal of Clinical Investigation, 89*, 1988-1994.

Gourgoulianis, K. I., Chatziparasidis, G., Chatziefthimiou, A., & Molyvdas, P. A. (2001). Magnesium as a relaxing factor of airway smooth muscles. *Journal of Aerosol Medicine, 14*(3), 301-307. doi: 10.1089/089426801316970259

Gray, H. (1918). *Anatomy of the Human Body* (20th ed.). Philadelphia: Lea & Febiger.

Healthcare, K. (2013, 11 Feb 2013). 4200 Standard | Montgomery Safe-T-Tube | Stents | Specialised Airway Management | Kapitex Healthcare Limited., from <http://www.kapitex.com/specialised/stents/montgomery-safe-t-tube/4200-standard/>.

Ho, A. S., & Koltai, P. J. (2008). Pediatric tracheal stenosis. *Otolaryngologic Clinics of North America, 41*(5), 999-1021.

Hoffer, M. E., Tom, L. W. C., Wetmore, R. F., Handler, S. D., & Potsic, W. P. (1994). Congenital tracheal stenosis: the otolaryngologist's perspective. *Archives of Otolaryngology, Head & Neck Surgery, 120*(4), 449.

Jacobs, J. P., Quintessenza, J. A., Botero, L. M., van Gelder, H. M., Giroud, J. M., Elliott, M. J., & Herberhold, C. (2000). The role of airway stents in the management of pediatric tracheal, carinal, and bronchial disease. *European Journal of Cardiothoracic Surgery, 18*(5), 505-512.

Ji, L. L. (1999). Antioxidants and Oxidative Stress in Exercise (44453). *The Society for Experimental Biology and Medicine, 222*, 283-292.

Jones, A. M., & Harrison, R. M. (2004). The effects of meteorological factors on atmospheric bioaerosol concentrations—a review. [doi: 10.1016/j.scitotenv.2003.11.021]. *Science of The Total Environment, 326*(1–3), 151-180.

Kippler, M., Bakhtiar Hossain, M., Lindh, C., Moore, S. E., Kabir, I., Vahter, M., & Broberg, K. (2012). Early life low-level cadmium exposure is positively associated with increased oxidative stress. [doi: 10.1016/j.envres.2011.11.012]. *Environmental Research, 112*(0), 164-170.

Kirkland, N., Birbilis, N., & Staiger, M. (2011). Assessing the corrosion of biodegradable magnesium implants, A critical review of current methodologies and their limitations. *Acta Biomaterialia*.

Knox, A. J., & Tattersfield, A. E. (1995). Airway smooth muscle relaxation. *Thorax, 50*(8), 894-901.

Ko, P. J., Liu, C. Y., Wu, Y. C., Chao, Y. K., Hsieh, M. J., Wu, C. Y., . . . Liu, H. P. (2009). Granulation formation following tracheal stenosis stenting: influence of stent position. [Comparative Study Research Support, Non-U.S. Gov't]. *Laryngoscope, 119*(12), 2331-2336. doi: 10.1002/lary.20615

Kourie, J. I. (1998). Interaction of reactive oxygen species with ion transport mechanisms. *American Journal of Physiology - Cell Physiology, 275*(1), C1-C24.

Kumar, A., & Ghosh, B. (2009). Genetics of asthma: a molecular biologist perspective. *Clinical and Molecular Allergy, 7*(1), 7.

Kumar, V. (2010). *Pathologic Basis of Disease* (8th ed.). Philadelphia: Elsevier.

Leonard, P. (1997). *Building a Medical Vocabulary* (4th ed.). St. Louis: Library of Congress.

Li, Z., Gu, X., Lou, S., & Zheng, Y. (2008). The development of binary Mg-Ca alloys for use as biodegradable materials within bone. [Journal Research Support, Non-U.S. Gov't]. *Biomaterials, 29*(10), 1329-1344.

Luckey, T., & Venugopal, B. (1977). Metal Toxicity in Mammals, Volume 1: Physiologic and Chemical Basis for Metal Toxicity. *Metal toxicity in mammals. Volume 1. Physiologic and chemical basis for metal toxicity.*

Lunn, W., Feller-Kopman, D., Wahidi, M., Ashiku, S., Thurer, R., & Ernst, A. (2005). Endoscopic removal of metallic airway stents. [Comparative Study]. *Chest, 127*(6), 2106-2112. doi: 10.1378/chest.127.6.2106

Marieb, E. (2010). *Human Anatomy and Physiology* (8th ed. Vol. San Fransisco): Pearson.

Medical, I. (2013). Hood Laboratories Hood Stoma Stents Straight with Plug Silicone 11mm O.D 22mm L, Made of Medical-Grade Silicone, Nonirritating To the Skin.

Michel, O. (2000). Systemic and local airways inflammatory response to endotoxin. [doi: 10.1016/S0300-483X(00)00288-2]. *Toxicology, 152*(1–3), 25-30.

Murphy, M. P. (1999). Nitric oxide and cell death. *Biochimica et Biophysica Acta (BBA)-Bioenergetics, 1411*(2), 401-414.

Noppen, M., Meysman, M., Claes, I., D'Haese, J., & Vincken, W. (1999). Screw-thread vs Dumon Endoprosthesis in the Management of Tracheal Stenosis*. *CHEST Journal, 115*(2), 532-535. doi: 10.1378/chest.115.2.532

NOVATECH. (2013). Dumon™ Tracheal and Bronchial Stents / Pulmonology / Boston Medical Products Inc.. from <http://www.bosmed.com/pulmonology/novatech-dumontm-tracheal-and-bronchial-stents.html>.

Pahl, H. L. (1999). Activators and target genes of Rel/NF-kappaB transcription factors. *Oncogene, 18*(49), 6853-6866. doi: 10.1038/sj.onc.1203239

Patel, B. D., Welch, A. A., Bingham, S. A., Luben, R. N., Day, N. E., Khaw, K. T., . . . Wareham, N. J. (2006). Dietary antioxidants and asthma in adults. [Journal Research Support, Non-U.S. Gov't]. *Thorax, 61*(5), 388-393.

Patel, R. P., McAndrew, J., Sellak, H., White, C. R., Jo, H., Freeman, B. A., & Darley-Usmar, V. M. (1999). Biological aspects of reactive nitrogen species. *Biochimica et Biophysica Acta, 1411*(2-3), 385.

Poynter, M. E., Irvin, C. G., & Janssen-Heininger, Y. M. W. (2003). A Prominent Role for Airway Epithelial NF-κB Activation in Lipopolysaccharide-Induced Airway Inflammation. *The Journal of Immunology, 170*(12), 6257-6265.

Purnama, A., Hermawan, H., Couet, J., & Mantovani, D. (2010). Assessing the biocompatibility of degradable metallic materials: State-of-the-art and focus on the potential of genetic regulation. *Acta Biomaterialia, 6*(5), 1800-1807.

Rafanan, A. L., & Mehta, A. C. (2000). Stenting of the Tracheobronchial Tree. *Radiologic Clinics of North America, 38*(2), 395-408. doi: http://dx.doi.org/10.1016/S0033-8389(05)70170-6

Reed, C. E., & Milton, D. K. (2001). Endotoxin-stimulated innate immunity: A contributing factor for asthma. [doi: 10.1067/mai.2001.116862]. *Journal of Allergy and Clinical Immunology, 108*(2), 157-166.

Saito, Y., & Imamura, H. (2005). Airway stenting. [Review]. *Surg Today, 35*(4), 265-270. doi: 10.1007/s00595-004-2942-y

Song, G. (2007). Control of biodegradation of biocompatible magnesium alloys. *Corrosion Science, 49*(4), 1696-1701.

Staiger, M. P., Pietak, A. M., Huadmai, J., & Dias, G. (2006). Magnesium and its alloys as orthopedic biomaterials: a review. *Biomaterials, 27*(9), 1728-1734.

Theodore, P. R. (2009). Emergent Management of Malignancy-Related Acute Airway Obstruction. *Emergency Medicine Clinics of North America, 27*(2), 231-241. doi: http://dx.doi.org/10.1016/j.emc.2009.01.009

Valko, M., Rhodes, C. J., Moncol, J., Izakovic, M., & Mazur, M. (2006). Free radicals, metals and antioxidants in oxidative stress-induced cancer. *Chemico-Biological Interactions, 160*(1), 1-40. doi: S0009-2797(05)00433-3 [pii] 10.1016/j.cbi.2005.12.009

Waterman, J. T., & Adler, K. B. (2008). Oxidant Stress and Airway Epithelial Function. *Current Topics in Membranes, 61*, 243-255.

Waterman, J.T. , Watson, C.Y., Tatum, S.D., Xu, Z., Luffy, S., and Gilbert, T.W. (2012). Interactions between magnesium biomaterials and differentiated human tracheobronchial epithelial cells. *American Journal Respiratory Critical Care Medicine* 185, A6346.

Weishaupt, K. R., Gomer, C. J., & Dougherty, T. J. (1976). Identification of singlet oxygen as the cytotoxic agent in photo-inactivation of a murine tumor. *Cancer Research, 36*(7 Part 1), 2326-2329.

Witte, F., Hort, N., Vogt, C., Cohen, S., Kainer, K. U., Willumeit, R., & Feyerabend, F. (2008). Degradable biomaterials based on magnesium corrosion. *Current Opinion in Solid State and Materials Science, 12*(5), 63-72.

Xin, Y., Hu, T., & Chu, P. K. (2011). *In vitro* studies of biomedical magnesium alloys in a simulated physiological environment: a review. [Journal Research Support, Non-U.S. Gov't Review]. *Acta Biomaterialia, 7*(4), 1452-1459.

Xin, Y., Huo, K., Tao, H., Tang, G., & Chu, P. K. (2008). Influence of aggressive ions on the degradation behavior of biomedical magnesium alloy in physiological environment. *Acta Biomaterialia, 4*(6).

Yuen, C., & Ip, W. (2010). Theoretical risk assessment of magnesium alloys as degradable biomedical implants. *Acta Biomaterialia, 6*(5), 1808-1812.

Zakaluzny, S. A., Lane, J. D., & Mair, E. A. (2003). Complications of tracheobronchial airway stents. [Review]. *Otolaryngol Head and Neck Surgery, 128*(4), 478-488.

Zhang, S., Zhang, X., Zhao, C., Li, J., Song, Y., Xie, C., . . . Bian, Y. (2010). Research on an Mg-Zn alloy as a degradable biomaterial. [Journal Research Support, Non-U.S. Gov't]. *Acta Biomaterialia, 6*(2), 626-640.

Appendix A

Protocols

Protocol #1: RNA Extraction

Qiagen RNA extraction kit was used

<u>**Before starting**</u>

1. Ensure that 10 μl β-ME/1ml Buffer RTL has been added.

2. Ensure that ethanol has been added to Buffer RPE (before initial use).

3. If performing on column DNase digestion protocol, prepare DNase I stock solution.

   [10 μl DNase I Stock + 70 μl Buffer RDD = 80 μl/rxn]

4. During procedure, work quickly (at RT).

For animal cells grown in a monolayer (do not use more than 1 x 10^7cells). Cells grown in a culture dish may be lysed directly, but cells grown in a flask must be trypsinized and collected in a microfuge tube.

<u>**To Lyse Cells**</u>

1. Aspirate media.

2. Add Buffer RTL→ Dish diameter <6 cm^2 (12-well dish) = 350 μl; 6-10 cm^2 (6-well dish)= 600 μl

3. Collect cell lysate with a cell scrapper (rubber policeman).

4. Pipet lysate into a microfuge tube and vortex to remove clumps.

5. Homogenize cells by passing lysate at least 5 times through a 20-gauge (0.9 mm diameter) fitted RNase-free syringe (alternatively add lysate to a QIAshredder spin column fitted with a 2 ml collection tube and spin a max speed for 2 min).

6. Add 1 volume (usually 350 or <u>600 μl</u>) of 70 % EtOH to the homogenized lysate and mix by pipetting.

7. Add up to 700 μl of the sample (including any ppt.) to RNeasy spin column fitted with a 2 ml collection tube. Close tube gently.

8. Spin for 15 sec at ≥8000g (≥10,000 rpm) to wash column. Discard flow-through and collection tube.

On-Column DNase I Digestion

D1. Add 350 μl RW1 to the column and spin 15 sec at ≥8000g (≥10,000 rpm) to wash column.

D2. Add 80 μl DNase mix to the center of each silica-gel membrane. Incubate at RT for 15 min.

D3. Add 350 μl RW1 to the column and spin 15 sec at ≥8000g (≥10,000 rpm) to wash column.

Wash and RNA Elution

9. Add 500 μl Buffer RPE onto column. Close gently.

10. Spin for 15 sec at ≥8000g (≥10,000 rpm) to wash column. Discard flow-through.

11. Add another 500 μl Buffer RPE onto column. Close gently. Spin for 15 sec at ≥8000g (≥10,000 rpm).

12. To dry column, spin at max speed for 1 min.

13. To elute, transfer column to a 1.5 ml microfuge tube and add 50 µl RNase-free water

    directly to the silica-gel membrane. Close gently.

14. Spin for 1 min at ≥8000g (≥10,000 rpm).

Determine RNA concentration and purity

1. Dilute RNA 1/50 (1 µl sample + 49 µl water).

2. Measure A_{260}.

    $A_{260} = 1 \rightarrow 40$ µg RNA/ml

    [RNA Sample] = 40 µg /ml x A_{260} x dilution factor

Store RNA at -70°C or proceed with cDNA synthesis.

iScript^{TM} cDNA Synthesis Kit (BIO-RAD)

Component	Volume per reaction
5x iScript Reaction Mix	4 µl
iScript Reverse Transcriptase	1 µl
Nuclease-free water	x µl
RNA template* (100 fg to 1 µg Total RNA)	x µl
Total Volume	20 µl

Reaction Protocol

Incubate complete reaction mix:

Step 1 5 min @ 25°C

Step 2 30 min @ 42°C

Step 3 5 min @ 85°C

Step 4 Hold @ 4°C (optional)

*When using larger amounts of input RNA (> 1μg) the reaction should be scaled up, e.g. 40 μl

for 2 μg, 100 μl for 5 μg to ensure optimum synthesis efficiency.

Protocol #2: RNA Quantification

(NanoDrop 2000 Spectrophotometer)

1) Open the NanoDrop application on the laboratory computer

2) Select the nucleic acid protocol

   a) Change the units to ng/ μL

   b) Change from DNA to RNA

3) Clean the NanoDrop with ethanol

   a) Clean the NanoDrop between each sample as well

4) Use nuclease free water to blank the NanoDrop

   a) Pipette 1uL of nuclease free water directly onto the center of the NanoDrop sensor

   b) Close the top of the NanoDrop and click blank

5) Use the RNA concentration data sheet to record your values

   a) Clean the sensor with ethanol

   b) Place 1uL of RNA on the sensor

   c) Close the lid and click "measure"

   d) Repeat for all of your samples

Protocol #3: Reverse Transcriptase PCR
iScript Reverse Transcriptase kit was used

In the RNA hood:

1) Turn on the U.V. light for at least 15 minutes to sterilize all surfaces

    a) wipe all surfaces with ethanol and RNase zap

2) Using the sterile RNA hood, pipette the pre-calculated amount of 5x iScript mix, 1x RT

    (from kit), nuclease free water.

    i) To calculate the amount of RNA needed from each sample, you'll need to divide 500

       by the concentration

       (1) 500÷ RNA Concentration= μL of RNA sample needed

    ii) Each sample should have 20 μL total

       (1) The combined total of nuclease free water and RNA sample is 15.

          (a) The amount of nuclease free water is determined by the amount of RNA

             sample minus 15.

             (i) RNA sample - 15= μL of nuclease free water

       (2) You'll add 4 μL of 5x iScript to each reaction

       (3) You'll add 1 μL of 1x iScript RT to each reaction

       (4) E.g.

Sample #	RNA μL	Water (μL)	5x iScript (μL)	1x iScript (μL)
1	5.0	10.0	4.0	1.0
2	3.0	12.0	4.0	1.0

3) Place each tube into the iCycler PCR machine and run cDNA program found under waterman protocols

4) Remove at the end of the cycle and store in freezer @-20˚C.

Protocol #4: Polymerase Chain Reaction

1) Create a Mastermix for each primer using the following template:

   a) Creates only one reaction

      i) Multiply each value by the number of reactions you need

   b) Place cDNA in PCR tube, then add 23 µL of "mastermix"

cDNA Template	2µL
FWD-Primer	0.5 µL
REV-Primer	0.5 µL
2x GoTaq Green	12.5 µL
Total	25 µL

2) Add 23 µL of mastermix to each pre-labeled tube with 2 µL of cDNA template and in the no template tube.

3) Quickly pulse all tubes in shaker to pull all components down.

4) Using iCycler place all tubes in appropriate slots and be sure that all lids are secure and closed.

5) Log into iCycler and go to:

   a) Protocols

   b) Waterman

   c) Oxstress program

   d) Click "run"

      i) Change sample volume on run screen to 25 µL

   e) Begin run

6) At the end of the cycle press end hold on iCycler and to store freeze samples in -20˚C

    freezer.

Protocol #5: Agarose Gel

1) Weigh 1.0 gram of agarose on a weigh boat

2) Add 100 ml of TBS buffer in a flask (250ml) and add agarose

3) Microwave on high until there are bubbles (right before boiling) present

   a) Periodically stop the microwave and swirl solution noting the clarity each time (maybe

   two times)

   b) Continue to microwave until the solution is totally clear

4) Let the flask cool slightly (about 30 sec. to a minute)

5) Add agarose solution to gel casting site

6) Add 7 µL of marker (depending on which type of marker you choose to use) to lane 1 of your

   solidified gel

   a) Add marker in-between each set of samples you plan to run

7) Pipette 15 µL of sample in each well.

   a) If you've used the 51 well comb, place 10 µL of sample in each well

8) Start the gel at 80 volts to get the DNA out of the wells

   a) You may turn the voltage up to 120 volts for the remainder of the run

9) When the gel has run ¾ of the way down the gel stop it the run

10) Stain the gel with Ethidium Bromide for 15-20 minutes

   a) **Beware Ethidium Bromide is a carcinogen, use extreme caution with each use**

11) Image the gel following Ethidium Bromide staining

   a) Refer to protocol 6 for imaging

12) Clean all surfaces and dispose of gel in Ethidium Bromide gel biohazard waste.

Protocol #6: Bio-Rad Image Lab Gel Imaging Protocol

The Bio-Rad imager is designed to be on all the time. If the Imager is not on, the ON/OFF switch is located on the front of the imager in the right bottom corner.

1. Pullout the UV drawer located on the front of the imager.

2. Place your stained gel directly on the UV table and close the drawer.

    a. If you are imaging a protein blot, place the white light cover directly on top of the UV light table.

    b. Place the blot directly on the white light cover and close the drawer.

3. Open the "Image Lab" program on the laboratory computer located next to the imager.

4. When the "Start Page" dialogue box appears select new protocol.

    a. If the "Start Page" dialogue box does not automatically pop-up go to the tool bar and select "New Protocol" (it looks like a sheet of clean printer paper)

5. Select a single channel protocol

    a. Skip the imaging area section

    b. Select automatic or enter a manual exposure time

6. Select position gel (yellow box on the lower left-hand corner)

    a. Use the zoom function to resize the imaging box around your gel or blot.

7. Select Run Protocol

    a. Your image will be captured at this time

8. After the image has been saved, please remove the gel and clean the UV table with 70% Ethanol.

To perform densitometry on the bands:

9. Click the Lane and bands icon located in the left hand column named "Analysis Tool Box"

   a. For best results manually input the number of lanes that you will be detecting bands.

      i. You may use the automatic option, however there is a large chance that it may not detect all lanes.

10. Select the bands tab and click detect bands

    a. When the "band detection" dialogue box appears, select your preference in band detection sensitivity.

       i. Depending on your bands you may need to increase or decrease the detection sensitivity.

    b. Choose detect

       i. If all of your bands were not detected simply add them by clicking "add" and clicking on the band that was omitted.

       ii. If by chance there is a band detected and it is not a band you wish to analyze simply delete it by selecting "delete" and clicking on the unwanted band.

11. Located in the main tool bar select "Analysis Table"

    a. You will be able to see all relevant information for each lane and band detected.

b. You may export these files to Microsoft Excel

12. To save simply select "File" and "Save As"

i. Select the appropriate destination and save the file.

Protocol #7: Preparing Mammalian Whole Cell Extracts

1) Place cells on ice. Labeled microfuge tubes and place on ice.

2) Removed media from cells by vacuum-aspirating and washed gently with 1 ml cold PBS containing Phosphatase Inhibitor (1 ml aliquots at -20°C)

3) While on ice, add 100-200 μl ice-cold "Extraction Buffer" to each well (6 well plate)

   a) To make Extraction Buffer:

      i) Make 1X Cell Signaling Lysis Buffer

         (1) Obtain 10X CS LB Stock (500 aliquots at -20°C) dilute with 4.5ml-deionized water.

      ii) Add 870 μl 1X CS Lysis Buffer prepared from (i) to 100 μl 10X Roche® Complete Protease Inhibitor Cocktail Tablet aliquots (100 μl aliquots stored at -20°C, labeled "PIT").

      iii) Add 970 μl Pre-Extraction Buffer(ii.) to:

         (1) 10 μl Phosphatase inhibitor Cocktail 1(20 μl stored at 4°C)

         (2) 2. 10μl protease inhibitor cocktail 1(20 μl stored at -20°C)

4) Rock plates on ice and work one plate at a time.

5) Use a cell scraper to scrape wells to one side of the well.

6) Transfer this lysate to the adjacent well. (Clean cell scraper in between samples with 70% ethanol and wipe with a Kimwipe)

7) Transfer lysate to appropriate tube and return to ice

8) Sonicate 3 times for 7 second bursts with 1 minute incubations on ice

9) Pellet debris at 15,000 rpm at 4°C for 15 minutes

10) Transfer supernatant to a clean tube.

11) Determine protein concentration via Bradford Assay

Protocol #8: Microplate Bradford Assay

1) Use two (2) sets of BSA standards (800, 400, 200, 100, 50, 0 mg/ml) stored at 4oC.

2) Dilute the Bradford Reagent Assay Dye (stored at 4oC) 1:4 in dH20.

3) Prepare a 1:100, 1:200 and 1:300 dilution of each unknown sample in triplicate.

4) Add 10 µL BSA standards, 10 µL unknown sample dilutions (in triplicate).

5) Add 190 µL diluted Bradford Assay Dye to each sample well.

6) Read plate using plate reader.

   a) Turn on VersaMax Microplate Reader and put plate in drawer. Press "Drawer" button to open/close drawer.

   b) Click "SoftMax Pro v5" icon.

   c) Go to "Protocols" drop-down menu.

   d) Go to "Protein Quant."

   e) Go to "Bradford."

   f) Click "Template" to enter plate/sample information (i.e., Standard ID, Unknown Sample ID…).

   g) Click "Read."

   h) When finished, save and print results & standard curve

   i) MAKE SURE DRAWER IS CLOSED & COVER INSTRUMENT.

Protocol 9: Western Blot

<u>SDS-PAGE Analysis</u>

1. Added sample buffer to each extract (1/4 volume of 4X or ½ of 2X Laemmli Sample

   Buffer). Generally used 30-60 µg/ lane of cell extract for mini gels.

2. Boiled samples for 5 minutes.

3. Loaded samples onto SDS-PAGE gel.

4. Ran gel at 115 volts for 1 hour & 20 minutes at RT. (Run gels according to

   manufacturer's instructions).

<u>Semi-Dry Transfer</u>

1. Soaked 2 pieces of extra thick filter paper and one piece of nitrocellulose in Western

   transfer Buffer.

2. Made a sandwich (bottom to top) with 1 piece of filter paper, nitrocellulose, gel and 1

   piece of filter paper. Place in semi-dry transfer apparatus and run at 10 V for 30-60

   minutes.

<u>Wet Tank Transfer</u>

1. Presoaked 2 pieces of extra thick filter paper and one piece of nitrocellulose in ice cold

   transfer buffer.

2. Made sandwich with 1 filter pad, 1 piece of filter paper, nitrocellulose, gel, 1 piece of

   filter paper, 1 filter pad. Load into cassette and then into tank. Distribute ice around tank

   to keep temperature cool. Run gel at 100 V for 60 min.

<u>Blocking</u>

1. Nitrocellulose was removed from sandwich.

2. Blot was placed in 5% milk blocking solution and rocked at room temperature for one hour.

3. Blot was washed with TBS-T for 15 minutes with gentle agitation and washed twice for 5 minutes with gentle agitation.

Primary Antibody

1. Diluted appropriate antibody in TBS-T plus 0.5% BSA. Generally used 1:1000 (i.e. 10 μl antibody in 10 ml TBS-T/albumin).

2. Incubate blot overnight at 4ºC with agitation.

3. Blot was rinsed the following morning with TBS-T for 15 minutes once and washed twice for 5 minutes with TBS-T.

Secondary Antibody

1. Diluted secondary antibody in TBS-T plus 0.5% BSA. Generally used 5μl in 10 ml.

2. Incubated blot for one hour with agitation at room temperature.

3. Blot was washed with TBS-T for 15 minutes with gentle agitation and washed twice for 5 minutes with gentle agitation.

ECL Detection

1. Mixed equal amounts of ECL detection reagents (1-2 ml each per blot). It should come to room temperature before use.

2. Pipetted reagent over entire surface of membrane. Incubated for one minute.

3. Wicked excess liquid off by using dry edge of kimwipe.

4. Membrane was placed in sheet protector.

5. Exposed film to membrane. Exposure times vary depending on antibody and protein source.

Automated Film Development

1. Made developer and fixer. After use wrap container in foil.

    a. Developer

        i. 800 ml warm tap water

        ii. 200 ml developer

        iii. Pour into flask and swirl

    b. Fixer

        i. 720 ml warm tap water (16ºC to 27ºC)

        ii. 250 ml rapid fixer (solution A)

        iii. 30 ml hardener (solution B)

        iv. Pour into flask and swirl

2. After exposure, film was run through Hope Autovisualizer Processor.

Protocol #10: Growing NHBE Cells
(Modified protocol of Dr. Kimberly L. Raiford)

NOTE: Always use sterile technique while performing tissue culture procedures. Refer to "SOP for Sterile Technique and Tissue Culture Equipment" document for details.

Day 1: Seeding Cells

1. Select plate type 6-well (plastic only/transwell insert-for going to air).

2. Label plate(s) with Name, Date, Plate # and donor (e.g. 3T0025).

3. **Make collagen** solution to coat wells by diluting collagen stock in 0.02 N Glacial Acetic Acid.

    a. Collagen Stock Solution: 3.13 mg/ml $\cong$ 3.13 μg/μl

    b. Desired final concentration = 50 μg/ml

    c. 50/3.13 = 15.97 $\therefore$ use 16μl collagen stock/1 ml acetic acid.

4. Add 0.5 ml/well and swirl plate to achieve complete well coverage.

5. Let stand at <u>RT for 1 hour</u>.

6. Vacuum-aspirate excess collagen solution and wash wells with 1 ml PBS for <u>10 min at RT</u>.

7. Remove PBS and add 2 ml of conditioning media (50:50 without additives).

    a. **Preparing 50:50 Media (viable for 6 weeks @ 4°C)**

        i.   Obtain a T-75 tissue culture flask (#3275)

        ii. Obtain BEBM & DMEM and mark fluid level in BEBM bottle

        iii. Pour 250 ml of BEBM into flask and 250 ml of DMEM into BEBM bottle.

        iv. Add 250 ml of BEBM from flask to DMEM bottle.

        v.   Label accordingly with 50:50, initials, date and refrigerate.

8. Add 2 ml of conditioning media to wells and incubate @ <u>37°C/5% CO_2 for 1 hour.</u>

9. Add "2 ml/well" in 50 ml tube and "1 ml/well" in a 50 ml tube (to reconstitute cells for distributing into wells) and warm both tubes in 37°C water bath for 15-30 min.

    a. **Preparing Complete Media (viable for 6 weeks @ 4°C)**

        i. Get a "Clonetics BEGM Singlequots" pack (-20°C freezer in plastic bag).

        ii. Remove BPE & Retinoic Acid from Singlequots pack and place in "Extras" container in -20°C freezer.

        iii. Get Nystatin & BSA from -20°C freezer and BPE & Retinoic Acid (light sensitive, use small tubes) from the -70°C.

        iv. Thaw components at RT.

        v. Add all (11) components to 50:50 bottle, check them off on label from Singlequots pack and affix label to bottle, date, initial & refrigerate.

10. Determine how many vials of cells you will need (2.0 x 10^6 NHBE cells/vial) to seed the plates. Generally use ~ 1 x 10^4 cells/well (e.g., 3 6-well plates $\cong$ 18 wells = 13,888.88 cells/well). Record seed concentration.

    a. **Cells are kept in liquid nitrogen tank**.

    b. **Remember to mark log when you take cells!** (Box 5A)

        i. When retrieving LN_2-frozen cells get an ice bucket with lid. Tubes have been known to burst.

        ii. In hood, partially unscrew cap to make sure no LN_2 is in the threads of the vial. The close tightly again.

        iii. Quickly thaw cells for <u>1 min in 37°C</u> water bath.

iv. Add cells to pre-warmed tube with "1 ml/well" volume. Pipet twice (gently) to mix.

11. Vacuum-aspirate conditioning media.

12. Add 2ml complete media to wells (use "2ml/well tube) first then add 1 ml cells to each well (or transwell chamber if "Going to Air").

13. Gently swirl plates to get even coverage of the wells. Incubate at 37°C/5% CO_2 ON.

Day 2: Feeding Cells

1. Pre-warm (37°C water bath) 3 ml/well complete media for <u>15-30 minutes.</u>

2. Vacuum-aspirate spent media.

3. Add 3 ml of media to each well (OR 2 ml to bottom + 1 ml transwell chamber if "Going to Air").

4. Gently swirl plates and place back in incubator.

5. Wait two days before feeding cells again. Then feed them daily/every other day until they reach 80-95% confluency (around ~Day 5-7 depending on initial seed concentration).

6. Proceed with experiments <u>OR</u> proceed to "Going to Air" protocol.

Day 7: Going to Air

1. Vacuum-aspirate media.

2. Add 2 ml pre-warmed media to the bottom of well only. Gently swirl plates and return to incubator.

3. **Cells must be fed every day at this point.**

50:50 Media with Additives ≅ Complete Media Components

Additive	Stock Conc. (M/H)	Volume*	Final Conc.
Nystatin (in-house, -20°C)	22,000 U/ml	0.5 ml	22 U/ml
BSA (in-house, -20°C)	1.5 mg/ml	0.5 ml	1.5 µg/ml
Gentimicin (C.Sq.)	50 mg/ml	0.5 ml	50 µg/ml
BPE (in-house, -70°C)$^\epsilon$	13 mg/ml (65mg)	1 vial	0.13 mg/ml
Insulin (C.Sq.)	5 mg/ml	0.5 ml	5 µg/ml
Triiodothyronine (C.Sq.)	6.5 µg/ml	0.5 ml	6.5 ng/ml
Hydrocortisone (C.Sq.)	0.5 mg/ml	0.5 ml	0.5 µg/ml
rhEGF (C.Sq.)	0. 5 µg/ml	0.5 ml	0.5 ng/ml
Transferrin (C.Sq.)	10 mg/ml	0.5 ml	10 µg/ml
Epinephrin (C.Sq.)	0.5 mg/ml	0.5 ml	0.5 µg/ml
Retinoic Acid (in-house, -70°C	50 mM	0.5 ml	50 nM

*Aliquots (Clonetics SingleQuot and in-house) are prepared such that adding the entire volume of 1 tube/vial will yield the correct final concentration in 500 ml of 50:50 DMEM/BEBM Media.

$^\epsilon$If no in house BPE is available, use 2.5 vials of BPE from SingleQuot Bullet Kit.

C.Sq. = Clonetics SingleQuot, stored at -20°C in plastic storage bag

Protocol #11: NHBE Cell Harvest & Cryopreservation

1. Aspirate media, rinse T-75 flasks with 8-10 ml PBS buffer.

2. Added 6-8 ml of warm trypsin (thaw in 37°C water bath) to each T-75 flask. Incubated at 37°C for 5 min, rocking flask every 1-2 minutes or until most of the cells have detached.

3. Immediately added 5-10 ml of cold Trypsin Neutralization solution, serum-containing medium or pure serum to each flask.

4. Transferred cell suspension to a 50 ml conical tubes.

5. Rinsed flasks with 8-10 ml cold HBSS/ flask and added to conical tubes containing cell suspensions.

6. Centrifuged at 1250 rpm for 5 minutes at 4°C in an refrigerated Eppendorpf table top centrifuge.

7. Removed supernatant by gentle vacuum aspiration or pouring.

8. Tapped tube to remove clumps prior to adding media to cells.

9. Used ice-cold Expansion media (with high EGF, 25 ng/ml) to resuspend and wash cells. Pooled into one tube.

10. Centrifuged cells again at 1250 rpm for 5 minutes at 4°C.

11. Determine cell concentration and viability using Trypan Blue Exclusion Dye (20 μl dye + 20 μl cell suspension). Counted with Bio-Rad automated cell counter.

12. Resuspended cells to a concentration of 2.0×10^6-2.5×10^6 live cells/ml in Cell freezing Solution (80% BEBM expansion media, 10% DMSO; 10 % Heat inactivated FBS).

13. Made 1 ml cell aliquots. Using 2.0 ml cryotubes with internal threading and silicon gasket.

14. Placed cryotubes inside a cryopreservation cooler (purple rectangular or circle one); stored at -80°C, overnight.

15. Transferred cells to liquid nitrogen storage the next morning and recorded in LN2 logbook.

Appendix B

Posters and Title Page from Presentations

Biocompatibility of Magnesium-based Biomaterials for Airway Stent Applications

Tatum, SD[1,2,4], Watson, CY[1,3,4], Xu, Z[3,5], Luffy, S[4,6], Gilbert, TW[4,6], and Waterman, JT[1,4]

[1]Department of Animal Sciences, North Carolina A&T State University, Greensboro, NC, [2]Department of Biology, North Carolina A&T State University, Greensboro, NC, [3]Energy and Environmental Systems, North Carolina A&T State University, Greensboro, NC, [4]NSF-ERC Revolutionizing Metallic Biomaterials, North Carolina A&T State University, Greensboro, NC, [5]Department of Mechanical Engineering, North Carolina A&T State University, Greensboro, NC, [6]McGowan Institute for Regenerative Medicine, Departments of Surgery and Bioengineering, University of Pittsburgh, Pittsburgh, Pennsylvania

Biocompatibility of Magnesium-based Biomaterials for Airway Stent Applications

Tatum, SD[1,2,4], Xu, K[1,4], Watson, CY[1,3,4], Xu, Z[3,5], Luffy, S[4,6], Gilbert, TW[4,6], and Waterman, JT[1,4]

[1]Department of Animal Sciences, North Carolina A&T State University, Greensboro, NC, [2]Department of Biology, North Carolina A&T State University, Greensboro, NC, [3]Energy and Environmental Systems, North Carolina A&T State University, Greensboro, NC, [4]NSF-ERC Revolutionizing Metallic Biomaterials, North Carolina A&T State University, Greensboro, NC, [5]Department of Mechanical Engineering, North Carolina A&T State University, Greensboro, NC, [6]McGowan Institute for Regenerative Medicine, Departments of Surgery and Bioengineering, University of Pittsburgh, Pittsburgh, Pennsylvania